metals

MDPI

Review

Development and Performance of High Chromium White Cast Irons (HCWCIs) for Wear–Corrosive Environments: A Critical Review

Simbarashe Fashu and Vera Trabadelo *

High Throughput Multidisciplinary Research Laboratory (HTMR), Mohammed VI Polytechnic University (UM6P), Lot 660, Hay Moulay Rachid, Benguerir 43150, Morocco
* Correspondence: vera.trabadelo@um6p.ma

Abstract: There is a huge demand for high-performance materials in extreme environments involving wear and corrosion. High chromium white cast irons (HCWCIs) display better performance than many materials since they are of sufficient hardness for wear protection and can be tailored in chemical compositions to improve corrosion resistance; however, their performance is often still inadequate. This article reviews the chemical composition and microstructure design aspects employed to tailor and develop HCWCIs with combined corrosion and wear resistance. The performance of these alloys under wear and corrosion is reviewed to highlight the influence of these parameters in the industry. Existing challenges and future opportunities, mainly focusing on metallurgical alloy development aspects like chemical composition, casting, and heat treatment design, are highlighted. This is followed by suggestions for potential developments in HCWCIs to improve the performance of materials in these aggressive environments. Many variables are involved in the design to obtain suitable microstructures and matrix composition for wear–corrosion resistance. Computational modeling is a promising approach for optimizing multi-design variables; however, reliable field performance data of HCWCIs in wear–corrosion environments are still inadequate. Quantitative evaluation of the wear–corrosion performance of HCWCIs requires the development of laboratory and field tests using standard conditions like abrasive type and sizes, severity of loading, slurry velocity, pH, and temperature to develop wear–corrosion maps to guide alloy development.

Keywords: wear; abrasion; erosion; corrosion; microstructure; composition

check for updates

Citation: Fashu, S.; Trabadelo, V. Development and Performance of High Chromium White Cast Irons (HCWCIs) for Wear–Corrosive Environments: A Critical Review. *Metals* **2023**, *13*, 1831. https://doi.org/10.3390/met13111831

Academic Editor: Yugui Zheng

Received: 19 September 2023
Revised: 26 October 2023
Accepted: 27 October 2023
Published: 31 October 2023

Copyright: © 2023 by the authors. Licensee MDPI, Basel, Switzerland. This article is an open access article distributed under the terms and conditions of the Creative Commons Attribution (CC BY) license (https://creativecommons.org/licenses/by/4.0/).

1. Introduction

Material loss via wear is encountered in many processes, from earth movement, mining, mineral processing, slurry pumping, and machinery parts exposed to friction. Sometimes, the material under wear is also exposed to low pHs in an aqueous environment, for example, during wet grinding of sulfidic or phosphate ores and heavy pumping of acidic slurry containing hard particles [1–3]. It has been observed in studies by Jones [4] and Chelgani et al. [5] that combined wear–corrosion occurs even in neutral water during grinding in the presence of aeration. In such environments, the material media are exposed to harsh conditions because of the synergistic interactions between mechanical wear and corrosion, i.e., wear–corrosion [6–8]. Sometimes, abrasive particles accelerate wear–corrosion via repeated impact on the material, demanding materials with adequate impact toughness [9,10]. Thus, material design and selection become a difficult problem when wear and corrosion occur together. The best strategy in developing materials for such applications is to optimize mechanical strength and corrosion resistance [11,12]. Consequently, the material should be of sufficient hardness for wear protection and, at the same time, should contain enough elements like chromium (Cr), nickel (Ni), and molybdenum (Mo) in the matrix for corrosion resistance.

Figure 1 shows that iron-based metallic materials are commonly employed in applications involving wear; this is because of their combination of high strength and low cost. Depending on the carbon (C) content, these iron-based materials are classified as cast irons and steels.

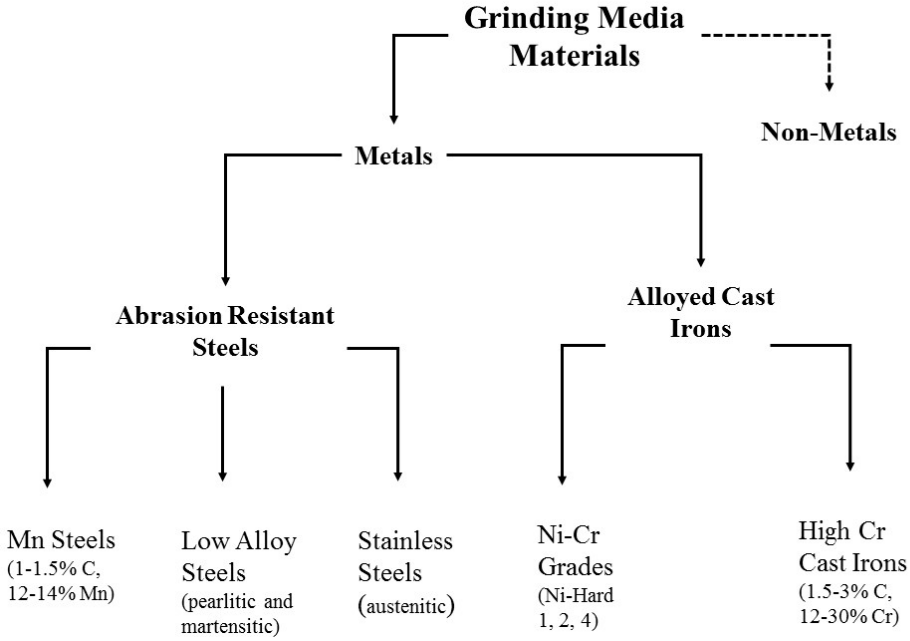


Figure 1. Common wear-resistant metallic materials employed during mining and comminution of ores. Reproduced with permission [13] 2013, Elsevier.

Among the alloys shown in Figure 1, high chromium white cast irons (HCWCIs) display great potential in wear conditions, for example, in wet grinding of ores. HCWCIs are cast irons containing >1.8 wt% C and >11 wt% Cr and may contain other alloying elements, for example, Mo, manganese (Mn), copper (Cu), and Ni. Their design and fabrication will be discussed in detail in Sections 3 and 4, respectively. Manganese (Hadfield) steels have a soft, ductile austenitic matrix and are applicable for rock mining because of their surface strain hardening on impact and high bulk impact toughness [14–17]. However, their drawbacks include low wear resistance compared to Ni-Hard/HCWCIs, low Cr contents to withstand corrosive environments, and they are relatively expensive to fabricate compared to HCWCIs [18]. Stainless steels are attractive because they have both good corrosion resistance and impact toughness; however, they are expensive and exhibit rapid wear in environments where wear dominates corrosion because of either the absence or low volume fraction of hard carbides in their microstructures [19,20]. Ni-hard alloys compete with HCWCIs in pure wear environments; however, they contain low Cr contents, making them inferior in environments where corrosion is aggressive [18,21]. Low alloy steels with pearlitic and martensitic microstructures contain low Cr contents to resist corrosive environments. They are mostly inferior to HCWCIs even in pure wear environments because of the low volume fraction of carbides [22]. Thus, steels and HCWCIs are potential materials for wear–corrosive environments, with steels being superior when corrosion dominates wear, while HCWCIs are superior when wear dominates corrosion [19]. Studies by Chenje et al. [22,23] show that HCWCIs perform better than steels and other materials like Ni hard alloys and forged and pearlitic steels in some environments such that they are replacing these materials. The wear–corrosion characteristics and costs of iron-based alloys shown in Figure 1 are compared in Table 1 to clearly demonstrate the superiority of HCWCIs in wear and corrosive environments [13].

Table 1. Comparison of the performance and cost of potential alloys used in wear–corrosion applications in mineral processing and mining applications.

Alloy	Wear Resistance	Corrosion Resistance	Toughness	Cost	References
Mn Steels	Moderate	Low	Very high	Moderate	[14–17]
Low Alloy Steels	Moderate	Low	Good	Fair	[13]
Stainless Steels	Good	Excellent	Good	Expensive	[19,20]
Ni-Hard grades	Good	Fair	Poor	Moderate	[18,21]
High Cr Cast Irons	Excellent	Moderate	Poor	Low	[13,24]

HCWCIs are cheap, flexible to design due to wide chemical compositions and heat treatment options, and are easier to manufacture than steels, although their main drawback is low impact toughness [18,24]. Potential applications of HCWCIs include wet ore grinding mill liners or mill balls grinding media and slurry pump materials for mineral processing industries. HCWCIs with an optimum volume fraction of carbides for hardness and adequate elements like Cr and Mo in the matrix for corrosion resistance, together with acceptable impact toughness, are suitable for specific wear–corrosion environments. However, the main problem is that improvement in wear resistance in HCWCIs compromises corrosion resistance and vice versa.

The objective of this article is to review the literature concerning metallurgical development and performance of HCWCIs for wear–corrosion environments, including wet grinding of ores and slurry pumping. Challenges being experienced in the development and performance of these alloys are highlighted, and potential improvements are discussed. The review starts with the discussion of wear–corrosion in Section 2 to explore loss mechanisms under low-stress and high-stress wear in corrosive environments. After appreciating the role of wear–corrosion in mineral processing, the design and fabrication approaches of appropriate HCWCIs for wet grinding of ores and slurry transport of acid slurry are then reviewed. Thus, the fundamental science of designing HCWCIs is presented in Section 3 before demonstrating fabrication aspects in Section 4. This is followed by a review of the performance of reported HCWCIs in selected wear–corrosion environments in Section 5. Finally, future challenges are outlined in Section 6 before concluding remarks are presented in Section 7.

2. Wear–Corrosion Mechanisms

Wear is the mechanical removal of material from the surface of a component and causes failure [25,26]. The main mechanical wear mechanism in mining and mineral processing is abrasion. Abrasive wear occurs when a sliding surface or sliding/inclined particles damage the surface via erosion, impact, scratching, grinding, and gouging [27]. Impact involves microcracking and delamination under impact (due to plastic deformation) followed by abrasive removal of material from the surface [27,28]. The schematic mechanisms of wear that are common in mineral processing are shown in Figure 2a. Wear–corrosion is the material loss from the surface due to synergistic/combined effects of wear and corrosion leading to severe damage when compared to the summation of the separate two [8]. Wear–corrosion depends on the tribological environment like the type of ore, relative motion of wear surfaces, loading conditions, ore hardness and mineralogy, grinding alloy metallurgy, passivity and adherence of corrosion products, slurry temperature, pH, and dissolved oxygen. Wear–corrosion synergism can be evaluated by comparing mass loss in pure wear, pure corrosion, and combined wear–corrosion; if damage due to combined wear–corrosion is greater than the sum of individual damages, then synergism is occurring [8,29]. Synergism, S, can be defined as the ratio of the total loss, t, to the sum of individual wear, a, and corrosion, c, as shown in Equation (1) [8].

$$S = \frac{t}{a + c} \quad (1)$$

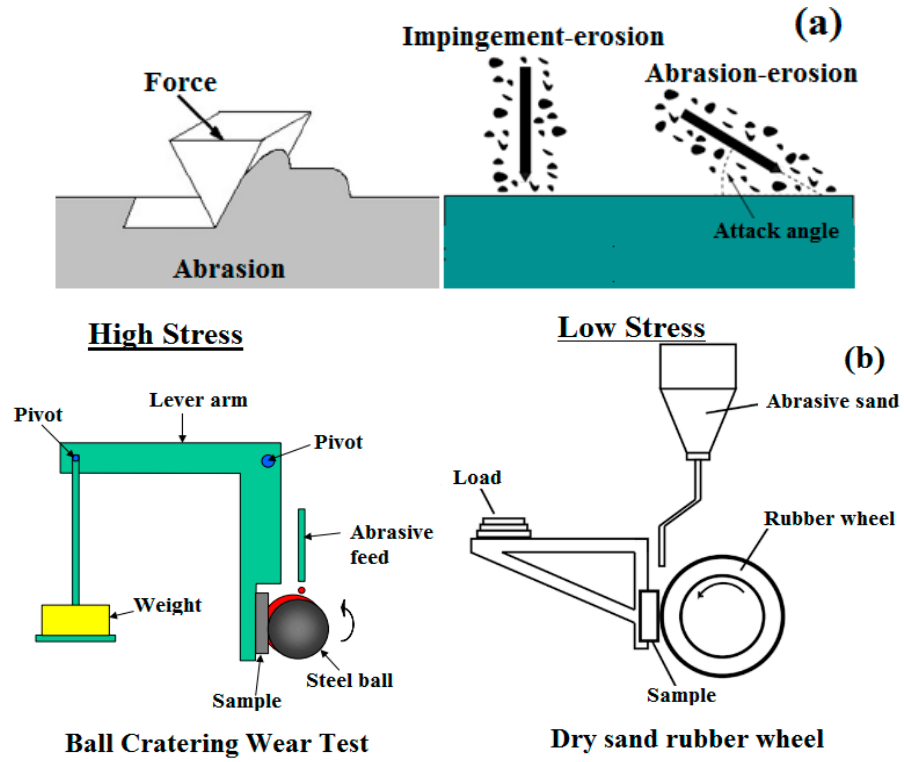


Figure 2. (**a**) Schematic illustration of common wear mechanisms; (**b**) Laboratory testing examples of high and low-stress wear–corrosion. Reproduced with permission [30] 2016, Elsevier.

The common mechanism of synergism in many passivating materials is the removal of passive films by wear followed by repassivation; therefore, the passive film should be hard and adherent to resist wear, and the metal should rapidly repassivate for corrosion protection [8]. To design and select appropriate materials for wear–corrosion environments, understanding the mass loss mechanisms occurring is important; therefore, this section briefly describes low-stress and high-stress wear–corrosion processes encountered in mineral processing. Figure 2b shows a schematic of low stress and high stress wear–corrosion, which can occur in the presence of a corrosive slurry.

2.1. Low Stress Wear (Erosion–Corrosion)

During the transportation of slurries in mineral processing, erosion–corrosion loss is accelerated by the repeated impact of the material surface by hard suspended solid particles in a moving fluid. The impact angle, impact speed, and properties of both material and slurry all influence material loss [31]. In most slurry transport cases, solid particle movement is almost parallel to the metal surface with a low angle resulting in low-stress erosion–corrosion, as shown in Figure 2b. This is because the load will not be sufficient to cause fracture of hard abrasive particles since they impinge on the metal surface at a low angle; therefore, the process is termed low-stress erosion–corrosion [32]. The process is characterized by continuous removal of the passive oxide film by hard particles in a moving slurry [19,31]. Laboratory erosion–corrosion evaluation of materials is usually performed using a slurry-pot tester schematically shown in Figure 3a [33]. In this tribological system, temperature, abrasive type, pH, dual samples, motor rotation speed, and impingement angle can be adjusted. An agitator can be placed below rotating samples to maintain the slurry in suspension. The material loss after a given period is determined using the formula given in Equation (2) [34].

$$Volume\ loss\left(\mathrm{mm}^3\right) = \frac{mass\ loss(\mathrm{g})}{density\left(\frac{\mathrm{g}}{\mathrm{m}^3}\right)} \times 100 \quad (2)$$

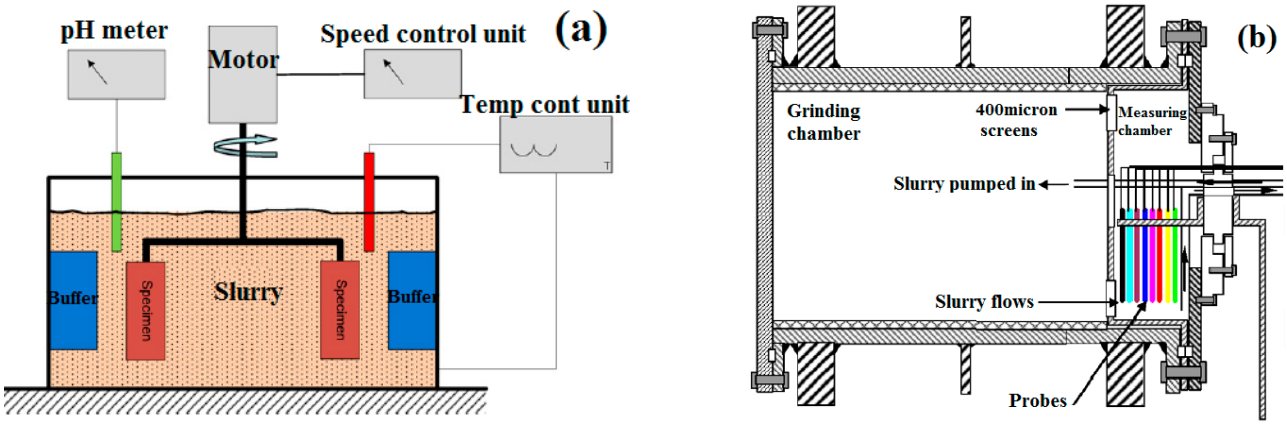


Figure 3. (**a**) Schematic illustration of the common slurry-pot abrasion–corrosion testing equipment; (**b**) laboratory ball mill test equipment used for wear–corrosion testing. Reproduced with permission [33,35] 2006, 2011, Elsevier.

2.2. High Stress Wear (Abrasion–Corrosion)

High-stress abrasion occurs when abrasive particles are fractured between two solid surfaces [6,36]. In wet grinding practice, high-stress abrasion occurs over a small region when ore particles are trapped between the grinding balls and the mill liner, and the load is sufficient to fracture abrasive particles (three-body abrasive wear) [37]. The high contact pressure produces indentations and scratching of the surface and pulverizes the abrasive ore particles such that wear of liners and grinding balls occurs by combined abrasion and corrosion [10,27,38,39]. Thus, wear of balls and liners is produced by combined cutting, plastic deformation, surface fracture, as well as tearing and spalling [40,41]. The impact is experienced as the balls cascade under the rotation action of the mill and contact the liners or ore, and this results in the appearance of micro cracks, which enhances wear. The mechanism of corrosion involves balls that become anodes, while oxygen reduction will be the supporting cathodic reaction [13,42]. Both low pH and high oxygen contents accelerate corrosion rate, and this is experienced when handling sulfidic ores [38,43]. Laboratory ball mills like the one schematically shown in Figure 3b are a reliable method for laboratory testing of high-stress wear using suitable operation variables [35]. In both high- and low-stress wear with corrosion, the designed alloy should combine adequate hardness and contain enough elements like Cr and Mo for rapid repassivation against corrosion. The optimum hardness and corrosion resistance depends on specific operating conditions, and alloy design and fabrication processes should be able to tailor the composition and structure suitable for a particular environment.

3. Design of Wear–Corrosion-Resistant HCWCIs

HCWCIs are used in environments containing different levels of mechanical wear with corrosion, for example, in ore crushing, ball milling, and slurry pumping. Some degree of impact is always experienced by components during service. HCWCIs should be designed to obtain the required properties using theoretical knowledge, literature data, and mathematical modeling.

3.1. Theory of High Chromium Cast Irons

The solidification behavior of HCWCIs should be properly understood to control and develop improved wear–corrosion-resistant materials. HCWCIs are developed from the Fe-C-Cr ternary system rich in iron (Fe); to obtain an austenite phase in HCWCIs, Cr content should be controlled between 11 and 30 wt% and C between 2 and 3.3 wt%, although this range can be shifted via the addition of other alloying elements. Thus, HCWCIs are alloys with Cr contents between 11 and 30 wt% and C contents above 2 wt% (cast iron) [43,44]. At Cr contents above 11 wt%, interconnected cementite (M_3C) in a pearlitic

matrix is replaced with strong rod or plate-like isolated M_7C_3 carbides. M stands for either Cr or Fe; Cr and Fe are usually mixed. The presence of strong and isolated M_7C_3 carbides improves the hardness, ductility, and toughness of the HCWCI. The term white cast iron originates from the presence of M_3C/M_7C_3 carbides characterized by a white appearance of the fractured surface [45]. HCWCIs solidify following the eutectic range marked by the line between austenite (γ) and carbides (M_7C_3). Once the eutectic is formed, it is also possible for the M_7C_3 carbides to react with the surrounding liquid to form M_3C carbides, which are thermodynamically stable and mostly appear as thin coatings surrounding M_7C_3 carbides [32,44,45] according to the reaction presented in Equation (3).

$$M_7C_3 + \text{Liquid} \rightarrow M_3C \quad (3)$$

Hypoeutectic HCWCIs have a composition range of 2–3.6 wt% C; eutectics contain around 3.6 wt% C, while hypereutectics contains above 3.6 wt% C. The solidification behavior of HCWCIs can be explained from the pseudo-binary phase diagram of the Fe-C-18Cr representative alloy calculated by the authors using ThermoCalc software and shown in Figure 4. Hypoeutectic alloys solidify by first forming primary austenite dendrites with a preferential growth direction accompanied by C and Cr solutes rejection into the melt. The last melt to solidify at the eutectic temperature/composition between austenite dendrites will be of eutectic composition and will solidify by the monovariant eutectic reaction to simultaneously form cellular colonies composed of layers of fine carbides and austenite according to the reaction shown in Equation (4) [32,46]:

$$L \rightarrow FCC(\gamma) + M_7C_3 \quad (4)$$

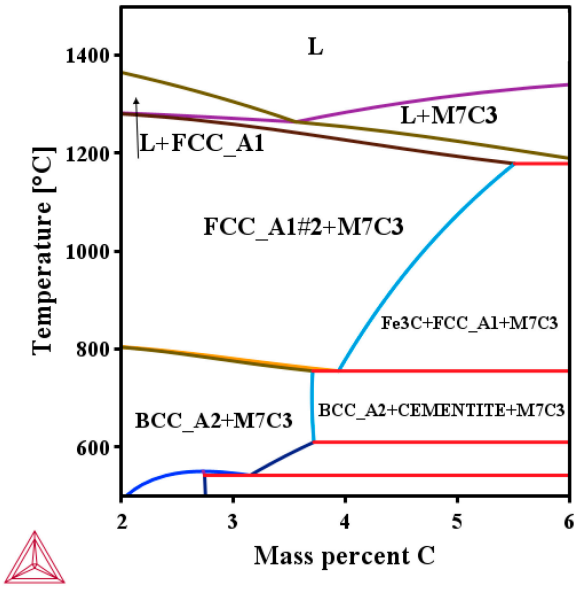


Figure 4. The Fe-C-18Cr phase diagram calculated by the authors using ThermoCalc Software (https://thermocalc.com/) showing phases stable under different temperatures and compositions.

M_7C_3 carbides are hard, and their formation reduces the C content of the matrix. The presence of high contents of Cr and C in primary austenite and fast solidification suppress its transformation to equilibrium pearlite (graphite +cementite), while in eutectic colonies, austenite cells will be surrounded by martensite [32,44,45]. This martensite develops when carbides form during eutectic reaction since eutectic austenite surrounding them will be deficient in C (due to carbide formation), so it will easily transform to martensite during cooling [32,47]. In addition to Cr and C, other hardening alloying elements like Ni, Mo, and Cu are often added.

Pearlitic matrix is not desired because it is brittle, contains low-hardness cementite carbides, and is of low corrosion resistance [48,49]. It can be observed from the phase diagram (Figure 4) that the solidification of hypereutectic HCWCIs commences with the precipitation of primary M_7C_3 carbides before the remaining liquid reaches the eutectic temperature to undergo a eutectic reaction. Thus, hypereutectic HCWCIs microstructures consist of a high-volume fraction of large, blade-shaped, and coarse primary carbides forming a continuous network within a eutectic colony such that the casting process is mostly characterized by a high scrap rate because the small volume matrix cannot support the carbides.

3.2. Chemical Composition Design

The chemical composition of HCWCIs should be optimized to obtain enough carbides for wear protection, and important elements should remain in the matrix for corrosion protection. The main alloying elements relevant for corrosion protection are Cr, Mo, C, and tungsten (W) [32,50]. The effect of main alloying elements on the wear and corrosion performance of HCWCIs is discussed in this section.

3.2.1. Carbon

In most situations, abrasion resistance increases with an increase in hardness, and accordingly, alloys are developed, assuming that wear resistance increases with an increase in bulk hardness [44,45,50]. It has been shown by Tang et al. [33,50] that abrasion resistance increases with an increase in carbon content up to 4 wt% (Figure 5) before decreasing because the smaller austenitic matrix will no longer be able to support a large volume of coarse carbides. Carbides decrease wear rate by hindering plastic flow during abrasion. However, fracture toughness rapidly decreases with an increase in carbide volume fraction. This is because of the low volume fraction of the austenite phase and the shorter paths for crack propagation [47,51]. The total carbide volume fraction (CVF) in HCWCIs mainly depends on C content and can be approximated using the Maratray [44,52] empirical formula shown in Equation (5).

$$\%CVF = 12.33\%C + 0.55\%Cr - 15.2 \quad (5)$$

Equation (5) shows that compared to C, Cr and other carbide formers have an insignificant influence on the total volume fraction of carbides (%CVF) [44]. To improve the fracture toughness of HCWCIs, a reduction in carbide volume fraction (reduced C content), carbide sizes, increase of intercarbide spacing and carbide hardness (add strong carbide formers nitrogen (N), W, vanadium (V)), and carbide spherodization have been attempted [32,53–55].

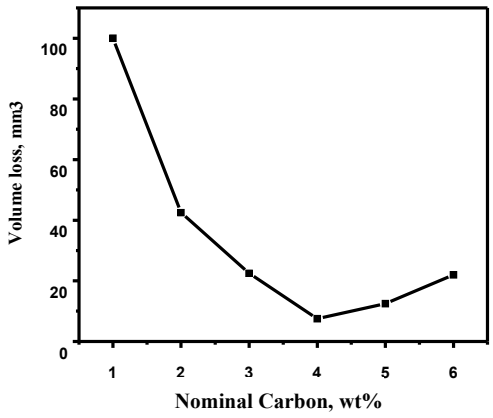


Figure 5. Influence of alloy carbon content on loss rate of HCWCIs in a wear–corrosion environment. Reproduced with permission [33] 2011, Elsevier.

3.2.2. Chromium

The Cr content of the as-cast austenitic matrix decreases with an increase in C content [44,56]. This is because Cr, compared to Fe, has a higher affinity for C such that most of it will report to carbides, increasing their hardness [32,57]. The Cr content in the matrix can be approximated using Equation (6) considering the nominal Cr content of the alloy (pct Cr) [57].

$$\%Cr_M = \frac{pctCr}{0.51 + 0.39\ pctC + 0.018\ pctCr} \quad (6)$$

The chromium content in the matrix increases with an increase in nominal Cr content but decreases sharply with an increase in C content because of its consumption in carbides. These relations show that under wear conditions in a corrosive environment, the addition of high Cr content is important to ensure that the matrix contains adequate Cr content. In stainless steels, the C content is maintained very low to ensure that Cr is not locked in carbides, while in cast iron, excess Cr must be added for a considerable amount to remain in the matrix for adequate hardness and corrosion protection [58,59]. Thus, the addition of strong carbide formers can enhance matrix Cr content by consuming some C [57]. HCWCIs with 30–45 wt% Cr demonstrating superior corrosion and wear resistance were successfully fabricated [33,50,60]; however, the main challenge is their low-impact toughness. Since the surface area of carbides (cathodes) will be large, while the matrix (anode) volume will be small at high carbide volume fractions, rapid localized corrosion will occur with an increase in C content in wear–corrosive environments [32,61]. Cr is readily passivating even under high-speed scratching, so after wear, the passive state reforms faster than it is removed in most environments [8,50,57,62]. Compared to those with lower Cr contents, higher Cr content WCIs of the same C content show high toughness due to grain refinement during solidification [50,51,63]. This is because high Cr content narrows the solidification range, as shown in computational thermodynamics calculations of the pseudo-binary phase diagrams of Fe-16Cr-C and Fe-26Cr-C alloys presented in Figure 6. An increase in nominal Cr content from 16 wt% to 26 wt% increases the eutectic temperature by approximately from 1285 °C to 1315 °C such that the solidification range decreases from 70 °C to 30 °C.

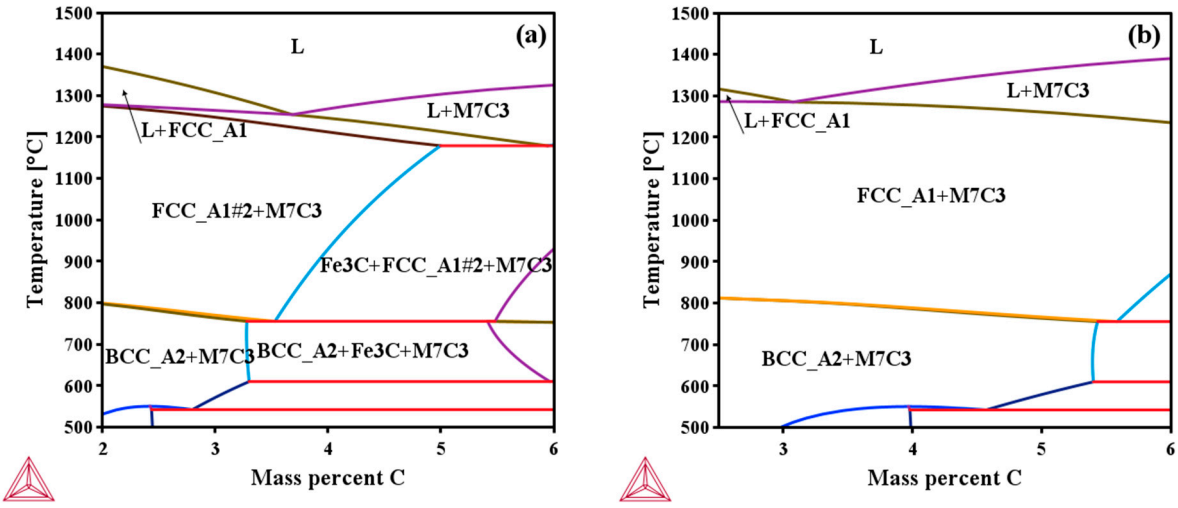


Figure 6. (**a**) Pseudo-binary phase diagrams for HCWCI alloys containing 16 wt% Cr; (**b**) 26 wt% Cr (calculated by the authors using the ThermoCalc software).

The corrosion resistance of an alloy is generally related to nominal Cr and C contents, as represented by Equation (7) [57].

$$\frac{R_P^0}{R_P} = exp\left[-0.011\left(\frac{pct\ Cr}{0.51 + 0.39\ pctC + 0.018\ pctCr}\right)^2\right] \quad (7)$$

where R^0_p is the polarization resistance when Cr content in the matrix is zero, R_p is the actual polarization resistance, and R^0_p/R_p is the corrosion resistance. Equation (7) shows that corrosion resistance increases with nominal Cr content and sharply decreases with an increase in C content. HCWCIs compositions with low C contents, i.e., hypoeutectic (1.8–3.6 wt% C), Cr contents between 12 and 30 wt% and carbides volume fraction >28 wt% are mostly used in wear–corrosion environments because their low volume fraction of carbides maintains high impact toughness while the presence of Cr ensures adequate corrosion resistance [11,57,64].

3.2.3. Alloying Elements Addition

In conventional HCWCIs, an increase in C content results in a high-volume fraction of carbides and low-impact toughness (and vice versa), making it difficult to optimize toughness and wear resistance simultaneously. Research on HCWCIs during the past decades has focused on the additions of alloying elements (one or more than one) to modify microstructures to improve hardness/wear resistance, impact toughness, and corrosion resistance. Since the main fabrication route of HCWCIs is melting and casting, these additions are mainly made by adjusting the quantity of the different ferroalloys added in the crucible to be heated in the induction furnace [49]. The main aim was to modify primary and secondary M_7C_3 eutectic carbide morphologies to globular shapes for enhanced impact toughness [65,66]. Alloying elements like V, W, titanium (Ti), and niobium (Nb) form hard MC carbides, where M is the element. In addition, alloying influences solidification and refines austenite dendrites and primary carbide sizes and morphology. The refining mechanism is influenced by MC carbide melting point and partitioning behaviors, which are summarized in Table 2.

Table 2. Crystal structure, melting point, and hardness of common carbides and the partitioning behavior of alloying elements between carbides and the ferrous matrix [49].

Carbide	Crystal Structure	Melting Point, °C	Max Hardness HV	Partitioning
$(Cr, Fe)_7C_3$	Hexagonal	1780	1800	-
$(Cr, Fe)_{23}C_6$	FCC	1520	1650	-
W_2C	Hexagonal	2750	2000	-
WC	BCC	2867	2400	Equal
VC	FCC	2830	2800	Equal
TiC	FCC	3150	3200	Zero
NbC	FCC	3490	2400	Zero

Ti and Nb form hard MC carbides, and they have an almost zero partition coefficient to the matrix [34,67,68]. Therefore, they reduce M_7C_3 carbides volume fraction by consuming C to form particles harder than M_7C_3, improving wear resistance and toughness in both austenitic and martensitic matrixes [32,44]. TiC and NbC have high melting points and are the first to precipitate from the liquid [45,69]. There are suggestions that they act as heterogeneous nucleation sites [45,69]. This theory is disputable because TiC carbides were observed either within the proeutectic matrix or attached to the eutectic carbides [51].

An acceptable explanation may be that large-sized TiC/NbC particles are engulfed by the advancing proeutectic austenite interface in a similar manner engulfment of dispersed ex situ particles occur during the manufacturing of metal matrix composites (MMCs) [70,71]. Then, both smaller TiC and solute particles are pushed by the interface, thereby retarding growth (refining morphology), and will appear and precipitate at the austenite/eutectic interface due to constitutional undercooling where agglomeration and clustering can occur. Particle engulfment or pushing depends on the interface velocity, which is influenced by the casting cooling rate. This is in agreement with explanations from some researchers who argue that the MC carbides cannot be nucleation sites since they have poor crystallographic fitting with the FCC austenite planes, and nucleation was only possible if the matrix was ferritic [32,45]. More studies on the development of microstructures in HCWCIs in the

presence of TiC/NbC particles are necessary using experimental and theoretical approaches like the phase field modeling [72,73] to obtain more insights into the actual physics. Although there are numerous studies on the addition of Ti and Nb carbides to improve wear via refining, all reports show that improvements in toughness are insignificant [74,75]. At a fixed C content, toughness/hardness increases with an increase in MC carbides up to a maximum value before decreasing since less hard rod/platelike M_7C_3 carbides will be replaced by harder globular particles before agglomeration occurs when MC carbides are in excess [74,75]. Via the consumption of C from the matrix during MC carbide growth, it was shown that the Cr content of the matrix is enhanced, and corrosion resistance is slightly improved [74,75]. The presence of fine dispersed MC carbides strengthens the matrix and improves wear performance by reducing plastic deformation and primary carbide cracking [18,76,77]. It was reported that the addition of Nb in hypereutectic HCWCIs can reduce the volume and refine and change the morphology of M_7C_3 eutectic carbides, making them more isotopic with enhanced fracture toughness [34,46,78]. Besides wear applications, improvement in toughness is also beneficial for machinability and extended tool life during machining.

W, Mo, and V carbides have lower melting points than TiC and NbC, and they can partition between the matrix and eutectic carbides, improving the hardenability of both phases [49,79–81]. Therefore, MC carbides are not easily formed at low contents of these elements; for example, in computational thermodynamics calculations for the pseudo-binary Fe-13Cr-3C-V phase diagram by Sanchez et al. [82], it was shown that VC precipitates from the melt only when V is in excess of 4.75 wt% V. The partitioning elements may also enrich the grain boundaries of M_7C_3 carbides to slow down growth in a preferential direction, change grain morphology, and enhance passivity [63,83]. V and boron (B) both reduce the solidification interval and refine M_7C_3 carbide and austenite dendrite arm spacing, increase the volume fraction of M_7C_3 carbides, and modify the morphology of carbides to enhance wear and toughness [84,85]. Carbides in the austenite matrix change from M_7C_3 to fine $M_{23}C_6$ with an increase in V and B due to enhanced nucleation rate such that toughness is enhanced [63,86]. Elements like B and silicon (Si) decrease C solubility in austenite and form a high-volume fraction of C nuclei and fine carbides. The partitioning elements Mo and W enhance secondary carbide precipitation in the austenite matrix during heat treatment to significantly improve wear resistance [32]. Nitrogen addition is another strategy for improving both the wear and corrosion resistance of HCWCIs [87–89]. The presence of nitrogen lowers corrosion potential, refine grain sizes, increases the content of carbides, and strengthens the matrix for enhanced corrosion and wear resistance [90,91]. However, several challenges are experienced in the introduction of alloying elements during foundry manufacturing of HCWCIs, including the high cost of alloy additions, oxidation of some elements like Ti, and technological difficulties in handling nitrogen.

3.3. Microstructure Design

After determining the matrix chemical composition for corrosion protection, the type of matrix should be designed to obtain the desired wear resistance. This is achieved via controlling casting and heat treatment fabrication parameters, as will be discussed in Section 4. A pearlitic matrix is soft to support carbides and has low corrosion resistance; therefore, it is not desired in severe wear–corrosive environments [8,22,44]. An austenitic matrix is soft, ductile, and tough and of high corrosion resistance; an as-cast HCWCI has an austenitic matrix. It cannot withstand severe abrasive conditions of microcutting and microploughing from hard abrasives, but at moderate abrasion/impact, its strain hardens to produce an alloy of high wear performance [8,32]. Austenite can accommodate high Cr contents above 12 wt% in an as-cast condition beneficial for enhanced corrosion resistance [8,32,57]. It was reported by some researchers that austenite transformation under impact stress promotes spalling and brittle fracture, while other researchers believe that the great plasticity of an austenitic matrix reduces damage generated under impact [32]. A martensitic matrix is hard and brittle such that it can easily withstand high wear conditions at low to moderate impact

stresses; martensite is obtained via heat treatment, as will be discussed in Section 4. The corrosion resistance of the martensitic matrix is lower than that of the as-cast austenitic matrix mainly because of its lower Cr and alloying elements content when the destabilization heat treatment is used. However, it is possible to obtain a martensitic matrix saturated with adequate elements for corrosion and abrasion resistance via alloying or cryogenic treatment of the as-cast alloy [32,92]. There are numerous controversies concerning the influence of austenitic and martensitic matrixes on wear rate, although it seems these contradictions emanate from simultaneous interactions of multiple variables, including abrasive type and size, stability of austenite, and loading stresses employed. It was reported by Zumelzu et al. [51] that martensite generally performs better with soft abrasives, while austenite is good with hard abrasives. Thus, the superiority of either austenite or martensite matrix mainly depends upon the wear mode [32,44]. In all cases, the austenite and martensite matrixes should be high in Cr content for corrosion protection.

3.4. Combined Composition-Microstructure Design

In HCWCIs exposed to corrosive-wear environments, the driving force for corrosion is the potential difference between carbides and the ferrous matrix. The ferrous matrix is the anode that corrodes, while carbides have higher corrosion potential and are the cathodes [61]. Failure of the matrix by corrosion means that the matrix will not be able to support carbides [8,61]. Lu et al. [57] developed a general wear/corrosion map where for good wear and corrosion resistance, the C content of the as-cast composition should be >2.2 wt% and Cr contents should be >22 wt%. However, synergistic wear–corrosion aspects were not considered in the development of this wear/corrosion map. Modeling methods [93] and Finite Element simulations [94] can be very valuable in helping overcome this existing difficulty in creating experimental wear maps.

In applications involving corrosion, high Cr contents of 25–30 wt% are normally used, while in purely abrasive conditions, Cr levels are mostly limited between 18 and 22 wt% [33,60]. This is in agreement with previous studies, which showed that in wear–corrosive environments, either low carbon contents (<3 wt%) or too high C contents (>6 wt%) resulted in serious wear–corrosion damage to HCWCIs [32,44,95]. Llewellyn [96] reported that if corrosion is significant, then a high Cr/C ratio should be considered. It should be noted that high Cr cast irons with 30–40 wt% Cr and low C contents of 1.5–2.4 wt% have an undesirable soft ferritic matrix that cannot strain harden during wear [11,60]. Austenite stabilizers like Ni are usually added to obtain pure austenite in these compositions [11,32,45].

4. Fabrication Approaches of Abrasion–Corrosion-Resistant HCWCIs

The processing of HCWCIs should be controlled to ensure that the desired microstructure with appropriate chemical composition distributions within the phases is obtained. Solidification and heat treatment are mainly used to fabricate HCWCIs and will be considered as the main fabrication routes. This section discusses the influence of casting and heat treatment variables on chemical composition and microstructure development.

4.1. Casting

The cooling rate during casting is mainly controlled by the type of mold used, i.e., sand, graphite, and metal. The microstructure, chemical compositions, and defects in HCWCIs are influenced by casting variables like superheat, inoculants additions, and solidification cooling rate [44]. Technologies like degassing and deoxidation are now widely employed to control defects. The effect of casting variables is discussed below to give some guidance on casting process design.

4.1.1. Cooling Rate

Fast solidification cooling rate refines grains and reduces carbide sizes; the final locations of MC carbides in the matrix also depend on the interface velocity, which is influenced

by the cooling rate. The cooling rate should be fast enough to avoid the formation of pearlite; additions of appropriate alloying elements like Mo, Ni, Mn, and Cu are sometimes used to stabilize the austenite phase in large castings [97,98]. In a study on the influence of cooling rate on wear resistance by Liu et al. [99], rapid cooling of 15 K/s refined the microstructure and increased hardness compared to a slow cooling rate of 1.5 K/s. However, the wear rate of as-cast samples with an austenite microstructure was almost similar independent of the hardness because the strengthening of all samples occurred via strain hardening and not grain refinement, although cracking of fine M_7C_3 carbides was experienced in a rapidly cooled alloy, showing that the slowly cooled alloy with coarse carbides was superior. In the heat treated martensitic matrix, the wear rate was less for the rapidly solidified sample, proving that the matrix could properly support small-sized carbides. It was shown in some studies that if carbide sizes are small, they can either break at high stresses or may be easily removed from the matrix [44,74]. The challenge with employing rapid cooling is that it cannot grain refine interiors of large components common in industry because of an inherent slow cooling rate at the center of the piece [44,100,101].

4.1.2. Superheat (Pouring Temperature)

Some researchers showed that large superheats resulted in coarse grains and carbides, thereby compromising toughness, corrosion, and wear resistance [44,101]. This is because of a large solidification range resulting in slow nucleation and cooling rates and elemental segregations. Thus, solidification will occur at higher temperatures, with slow nucleation accompanied by remelting and fast diffusion resulting in coarsening [32,47]. Therefore, nucleation should occur near the liquidus temperature for grain refinement to form an equiaxed morphology, but the main challenge is the increase in shrinkage porosity [102]. The appropriate superheat is selected based on the fluidity of the melt; thus, Si and manganese (Mn) are mostly added to enhance fluidity.

4.1.3. Inoculation

HCWCIs with high toughness and strength can be fabricated via a selection of appropriate inoculates with proper quantities. Grain refiners, for example, cerium (Ce) [103,104], strontium (Sr) [105], TiC [106], and ferrotitanium [107], are externally added to the melt as inoculations in HIWCIs and are effective in grain refinement via heterogeneous nucleation. Moreover, elements like B suppress C dissolution and enhance carbide precipitation from the melt to refine the melt. In this regard, they also act as inoculants [108]. Rare earths were also employed and proved to be effective modifiers [109,110].

4.1.4. External Forces

The application of external forces like mechanical, ultrasonic, electric pulse current, and electromagnetic vibrations in casting or mold during solidification causes a stirring of the melt, fragmentation, and nucleation [111,112], which control grain size and chemical segregation. In addition, external forces present in the selected casting method also affect grain refinement, e.g., centrifugal casting refines morphology better than sand casting. Grain refinement accompanied by mold vibration is attributed to either fragmentation of dendrite arms and high nucleation rate [113] or remelting [82,114] of dendrite necks due to stirring. An experiment on dynamic solidification [81] showed that sizes of the as-cast carbides were refined by solidification in the presence of mold vibration, enhancing the alloy hardness. An increase in vibration frequency enhanced microstructure refinement, alloy hardness, and impact toughness. In another study, the electric current pulse (ECP) method was employed and proved to be effective in breaking large clusters before solidification and dendrites during solidification to nucleate and refine the microstructure [115,116]. However, the challenge of the ECP method is the difficulty in applying it to large castings.

4.2. Heat Treatment

After the casting process, the HCWCIs can be used in the as-cast condition or are heat treated to modify the matrix microstructure depending on the intended application. Usually, the as-cast microstructure has a high content of Cr in the austenite matrix and is good for corrosion resistance but inferior in wear applications [51,56]. A destabilizing heat treatment is employed to destabilize the high alloy content austenite matrix at a temperature range of about 920–1060 °C for 1–6 h and transform it to martensite during cooling [32,56,76]. Transformation to martensite occurs because of secondary precipitation of carbides leaving an austenite matrix deficient in C and Cr, thereby increasing the martensite start (Ms) temperature; such that upon cooling, the matrix will transform to martensite with some retained austenite (about 35%). Soaking above 1100 °C mainly precipitates M_7C_3 carbides, while at below 1100 °C, a mixture of M_7C_3 and $M_{23}C_6$ is obtained [32,77,92]. Destabilization temperatures are mostly reached by first holding at intermediate temperatures to avoid cracking, especially when handling thick sections [32,77,92]. Pourasiabi and Gates [34] found that the presence of different sizes of carbides, i.e., primary and secondary, after heat treatment is beneficial in milling of different sizes of abrasives, i.e., coarse or fine ores. The martensite produced by destabilization is deficient in Cr and not suitable in wear–corrosion environments. The impact toughness of the quenched sample is finally improved by the tempering process; it is held at a low temperature, for example, at 200 °C for 2 h, to relieve stresses induced during transformation. Sometimes, the matrix with high martensite and low austenite content saturated with Cr can be developed for wear and corrosion applications, as discussed in Section 4.2.1. A typical complete heat treatment cycle is schematically presented in Figure 7.

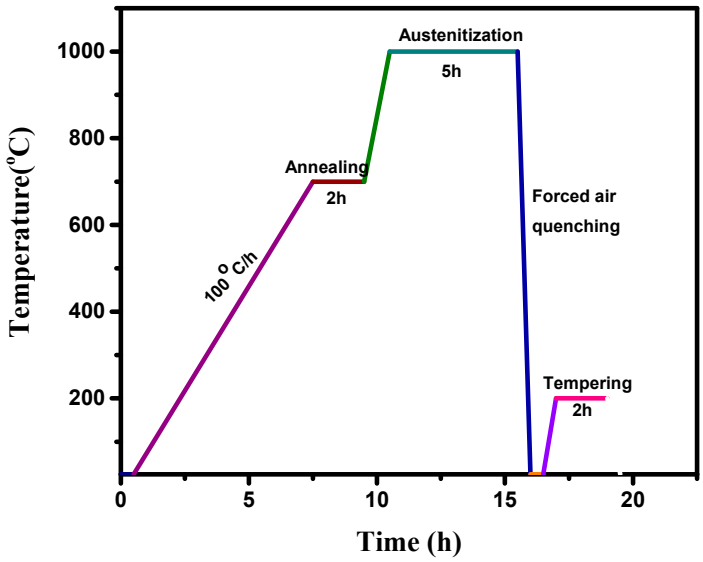


Figure 7. A typical complete heat treatment for HCWCIs showing the important main steps. Reproduced with permission [117] 2017, Elsevier.

4.2.1. Effect of Destabilization Temperature, Time, and Quenching Rate

Low destabilization temperatures cause extensive precipitation of secondary carbides consuming C and Cr from the austenite matrix, forming soft martensite, while very high temperatures will retain high C and Cr contents in the matrix to form hard martensite saturated in Cr with a high volume of retained austenite impairing hardness. In their work, Girelli et al. [118] investigated the influence of heat treatment on the corrosion performance of a 27%wt Cr HCWCI. It was shown that heat treating at a temperature of 1160 °C for 1 h significantly improved corrosion resistance by retaining high Cr content in the matrix because of high dissolution rates of carbides. Moreover, some investigators [92,119] reported that increasing austenitizing temperature decreased the hardness and wear resistance of

HCWCIs. An optimum destabilization temperature for required hardness (martensite content) and Cr content should be a temperature that is not too high to avoid much C and Cr dissolution in the matrix and not too low to avoid depleting all C and Cr from the matrix. Cryogenic treatment can be used after destabilization by cooling below the Ms temperature to reduce retained austenite levels to <5 wt%. Cryogenic treatments may also be used in as-cast austenitic structures by cooling them below Ms to eliminate destabilization, thereby avoiding stresses to enhance toughness [32,77]. In this way, high saturated C and Cr content can be maintained in the martensite for enhanced wear and corrosion resistance. Such innovative heat treatments show potential in the development of HCWCIs for wear–corrosion environments.

The effect of holding time on the hardness of HCWCIs shows that with an increase in holding time, the hardness increases up to an optimum before decreasing due to precipitation and coarsening of secondary carbides [32,47]. Prolonged holding times coarsen carbides via Ostwald ripening and reduce wear resistance [32,53]. Moderate cooling during quenching of destabilized austenite causes additional precipitation of secondary carbides, which is advantageous, while very slow cooling rates result in the formation of pearlite matrix with low hardness and corrosion resistance [120]. Very fast cooling is desirable but may cause cracking and residual stresses. The De-MQ-Sct process was proposed by Jia et al. [120] as an innovative destabilizing fast-cooling heat treatment that uses multi-cycle alternate water quenching and air cooling to reduce pearlite formation and enhance martensite content to obtain alloys with high hardness and toughness.

4.2.2. Effect of Alloying Elements

The influence of alloying elements on the heat treatment of HCWCIs was studied [80,121,122] using a hypoeutectic HCWCI, and the relationship between the number of alloying elements (Ni, V, Mo Cu) and hardness of retained austenite was established. Alloying elements, for example, Si, promote the decomposition of austenite by reducing C solubility in the austenite matrix, thereby raising the Ms temperature [32]. Elements that enhance C solubility retain more Cr in the matrix for corrosion protection, while those reducing C precipitation eliminate Cr from the matrix. Thus, alloying elements should be optimized to develop wear–corrosion-resistant HCWCIs. For example, at high C content, Cr in the matrix will be deficient, so alloying elements like Mo, Ni, and Cu should be added to prevent pearlite formation in favor of the austenite matrix [32].

4.2.3. Heat Treatment Design

The heat treatment of HCWCIs is difficult to optimize using trial and error approaches because of the multiple variables involved, including temperature, time, and cooling rates. Optimum values of parameters like destabilization temperature and holding times should depend upon the selected composition and must be properly determined. Many researchers used the same destabilization temperatures and holding times for alloys with different compositions, and such an approach does not lead to the fast development of HCWCI alloys. A few studies used computational modeling to optimize heat treatment parameters. Albertin et al. [11] used computational thermodynamics calculations to design the heat treatment parameters of wear-resistant HCWCI rings for the blast furnace feeding system. Other computational modeling approaches, including machine learning, demonstrate potential in designing HCWCIs since they can handle large volumes of data from composition selection, casting variables, and heat treatment to predict appropriate compositions, microstructures, and fabrication conditions [123,124].

Regarding computational thermodynamics, it has been proven to be a reliable tool for predicting the microstructure of HCWCIs [125,126]. It allows, for example, to evaluate the effect of the solutes on the formation of primary carbides during solidification [127]. Wang et al. [128] used computational thermodynamics to understand the mechanism for the formation of core–shell carbides in HCWCIs, while Pranav Nayak et al. [79] were able to successfully predict the eutectic carbide phase fraction in two HCWCIs.

5. Performance of HCWCIs in Wear–Corrosive Environments

The performance of HCWCIs in slurry pumping (low stress) and ball milling (high stress) in wear–corrosive environments depends on the hardness of the abrasives being handled. The selection of the abrasive material is very important in evaluating the performance of the materials because much harder abrasives tend to compress materials performances, classifying them to be of poor performance, while moderate abrasives can show clear differences in performances [129]. Wear occurs when the hardness of the abrasive is higher than that of the matrix because the abrasive will easily cut the matrix. Wear resistance is mainly dependent on the supporting effect of the matrix and the protective effect of carbides embedded in the matrix [32,44], while corrosion resistance is mainly influenced by the Cr content in the matrix and carbide volume fraction [51]. This section reviews wear–corrosion performances of HCWCIs during laboratory and field wet grinding (high stress) and during laboratory erosion–corrosion testing and slurry pumping (low stress) found in the literature to provide some insight for material development. Wear–corrosion tests were performed under different non-standard conditions such that comprehensive quantitative comparisons to demonstrate their effect on loss rates are impossible at this stage.

5.1. Low Stress (Erosion–Corrosion) Performance

In the presence of hard abrasives at low stress, increasing carbide volume fraction decreases wear rate because the matrix can support carbides since there are no severe deformation stresses to cause carbide cracking [32,57,119]. Martensite with low amounts of retained austenite and saturated with Cr performs better than austenite in moderate wear applications where austenite cannot strain harden [32,52]. Hardness values of most common abrasives are SiC (HV 2500–2600), alumina (HV 1800–2000) and silica (HV 900–1280) [32,45,49]. Most carbides like M_7C_3 (HV 1200–1800) have lower hardness values than these abrasives; therefore, because of low stresses, carbides are worn slowly and determine the overall wear rate [32,49]. However, for abrasives softer than austenite, an austenite matrix with high Cr content is superior because of its high corrosion resistance. Slurry erosion is caused by impingement of the surface by solid suspended particles resulting in material loss by repeated impact and is the main cause of failure in slurry pumping equipment. There is a strong erosion–corrosion synergy resulting in a high wear rate in this environment, as corroborated by the research by Tomlinson and Talks [130] and Kwok et al. [131] for wear–corrosion in brine solution.

5.1.1. Effect of HCWCIs-Abrasive Particles Interaction

Research by Al-Bhukaiti et al. [132] on the comparison of the influence of impingement angle on erosion–corrosion of steels and HCWCIs showed that HCWCIs exhibit high mass loss rates at higher impingement angles >45° due to carbides cracking and indentation of the matrix while at low angles the ductile matrix was deformed without fracture of carbides leading to low mass-loss rates. On the contrary, steel demonstrated high erosion rates at low angles due to high plastic deformation. In another work by Adler and Dogan [60], hypoeutectic HCWCIs showed higher resistance to erosion compared to a eutectic alloy because of the higher volume fraction of the austenitic matrix and corresponding high straining rates. Erosive wear occurs via the extrusion of thin platelets due to impact from eroding particles. High corrosion rates occurred at high volume fractions of carbides and larger erosive particle sizes since they exert high impact stresses. Yoganandh et al. [133] demonstrated that the erosion resistance of HCWCI is superior to that of CD4MCu duplex steel at both pH 3 and pH 7 under different impingement angles and velocities. Tian et al. [134] used Coriolis erosive wear tests to compare the performances of HCWCIs with aluminum alloys. The volume loss in HCWCIs was via sliding wear and low-angle impact fatigue cracking from solid particles, while aluminum loss rates were higher from sliding wear, cutting, and plowing mechanisms.

5.1.2. Effect of Chemical Composition

Chromium

Studies by Tang et al. [50] on microstructures and erosion–corrosion resistances of cast HCWCIs demonstrated that corrosion mainly depends on the matrix Cr content and carbide volume fraction (CVF), while erosion depends only on CVF. The erosion–corrosion performance of high Cr cast iron alloys in liquid–solid slurries was studied by Tian et al. [135]. The mass loss rates increased with slurry acidity, chloride content, and temperature. HCWCIs with high Cr content demonstrated high erosion–corrosion resistance. It was observed that in slurries with high pHs, erosion is the main mode of material removal, and loss rates increase with an increase in abrasive particle size. At low pHs, particles with sizes smaller than the average carbide spacing are more effective compared to larger particles in removing corrosion products and accelerating erosion–corrosion wear rate. Improvements in erosion–corrosion were achieved by reducing carbide-matrix hardness difference (via improving matrix hardness, e.g., either heat treatment or alloying), improving matrix corrosion resistance and macrohardness. Comparisons of the performance of HCWCI with steels were performed in a slurry pot at 45 °C in an aqueous slurry containing 35 wt% natural silica sand and 3.5 wt% NaCl by Islam et al. [31,136,137]. It was found that under that environment, HCWCIs did not have sufficient Cr in the matrix to withstand erosion–corrosion wear. The erosive-corrosion wear of two HCWCIs with different Cr/C ratios was tested by Salasi et al. [138] using three body tests under different electrolyte pHs and chloride contents with dispersed coarse garnet abrasive particles. Results showed that mass loss is high in most environments; the highest was observed at low pH, and the lowest was at high Cr/C ratios.

Carbon

Studies on erosion–corrosion wear of high carbon content HCWCI in the sand-containing water slurry showed an abnormal decrease in wear at a high C concentration of 6 wt% as water-sand slurry velocity increased from 2.5 m/s to 5 m/s, and this trend was reversed at low C concentration in hypoeutectic HCWCI [95]. The abnormal wear observed was attributed to competition between erosion and corrosion attack, where corrosion dominates at low velocities, and erosion dominates at high slurry velocities.

Molybdenum and Tungsten

Research on the influence of Mo on erosion–corrosion of as-cast HCWCIs in a sulfuric acid slurry with alumina particles was performed by Imurai et al. [139], and it was shown that erosion–corrosion resistance improves with an increase in Mo content. This was due to both the appearance of harder eutectic M_2C instead of the typical M_7C_3 carbides and the presence of adequate Mo in the matrix for corrosion protection. The influence of W during sand slurry erosion–corrosion of HCWCI was investigated by Wang et al. [140], and similar to Mo, a remarkable decrease in erosion–corrosion wear rate was observed with an increase in W contents.

Nitrogen

Erosion–corrosion wear behavior of a high nitrogen content HCWCI was studied by Lu et al. [88] in water-sand and acid-sand slurries. The wear resistance of nitrogen-containing HCWCI was 1.34 times higher than that of the base alloy without nitrogen. Improvement in performance was due to the dissolution of nitrogen in the matrix and the formation of carbon nitride to enhance corrosion and wear resistance. In another investigation by Xu et al. [87], the erosion–corrosion wear of high nitrogen HCWCI was 1.48 times higher than that of the base alloy without nitrogen. The erosion–corrosion resistance of nitrogen-containing alloy was probably higher because N improves the electrode potential, enhances self-repair of the passive film, and strengthens the matrix via grain refinement, precipitation, and solid solution hardening [87,88,90].

Rare Earths and Boron

In the work performed by Zhang and Li [141] on the influence of yttrium (Y) on erosion–corrosion behavior of 27Cr white cast iron, yttrium enhanced the surface passive film stability such that corrosion resistance increased with an increase in Y content up to 1 wt%. The explanation was that oxygen-active elements like yttrium and cerium are effective in enhancing passivity, while yttrium also enhances strength [62,104,141,142]. An HCWCI alloy with 35 wt% Cr and 3 wt% C was modified by adding traces of B in the matrix in research by Lu et al. [143], resulting in an improvement in carbide hardness and an increase in carbide volume fraction. Enhanced erosion–corrosion resistance was observed during alloy testing in a sand-containing slurry. The influence of B on erosion–corrosion behavior of 28%Cr white cast iron was studied by Naiheng et al. [144] at pH = 1 and pH > 3. B increases erosion–corrosion rate at low pH and improves erosion–corrosion resistance at high pH > 3. However, higher B contents were found to be detrimental in corrosion properties due to segregation and low matrix toughness.

5.1.3. Effect of Microstructure

Matrix

The erosion–corrosion wear behavior of HCWCIs (27 wt% Cr and 37 wt% Cr) were compared to their austenitic and martensitic counterpart steels using the submerged jet technique in a 3.5% NaCl electrolyte at pH 3 and pH 7 with silica particles in the slurry by Giourntas et al. [145] and Karafyllias et al. [146]. Austenitic alloys were superior in acidic conditions, while martensitic were excellent in neutral solutions. In an almost similar work, Al-Bukhaiti et al. [147] studied the erosion–corrosion wear behavior of an austenitic hypoeutectic and a martensitic near eutectic HCWCI with different C and Cr contents (Fe–27Cr–3C and Fe–37Cr-1.8C) and compared their performances with their stainless steel counterparts in a slurry electrolyte with angular silica particles and 3.5% NaCl under submerged jet impingement conditions. Both HCWCI and austenitic steels with high Cr contents were superior because of the presence of high Cr content in the matrix, and steel was superior. In a study by Gelfi et al. [148], two HCWCIs (14 wt% and 18 wt% Cr) and a Ni-hard alloy were exposed to different heat treatment conditions and tested for erosion–corrosion wear in flowing slurry using a modified-Coriolis apparatus. An HCWCI heat treated at (950 °C-2 h) exhibited superior wear resistance because of the presence of a hard martensitic matrix with fine secondary carbides, while the Ni-hard alloy was found to be good in the as-cast condition.

Comparison of HCWCIs with Other Materials

Low mass loss rates of slurry pump side liners using silica ores as abrasives were reported in Fe-27Cr-2.8C HCWCI compared to the high losses observed in natural rubber and grey cast iron by Walker et al. [149,150]. Llewellyn et al. [96] ranked different hypoeutectic and hypereutectic HCWCIs used in the manufacturing of pumps against steel in sand slurry during the Coriolis erosion–corrosion test and the performance of hypereutectic alloys was superior. In another study by Xie et al. [151], slurry sliding tests were used to study different materials, including steels and HCWCIs. High wear resistance was observed in HCWCIs due to the high-volume fraction of carbides. The differences were attributed to the different wear mechanisms encountered in laboratory tests compared to field tests. Jones and Llewellyn [152] employed slurry pot tests to study erosion–corrosion of a range of ferrous-based materials in an aqueous slurry with 3.5 wt% NaCl and 35 wt% silica. Results showed that HCWCIs exhibited the highest erosion–corrosion resistance. HCWCIs and high C steel grinding balls were tested for erosion–corrosion wear by jet slurry impingement with quartz and chalcopyrite slurries at various pH values in a study by Pitt et al. [153]. Strong synergism between corrosion and wear was observed, and steels performed better at low pH, while HCWCIs were good at high pH and severe wear conditions.

5.2. High Stress (Abrasion–Corrosion) Performance

Under high-stress abrasion, the relative hardness of the abrasive particle to the matrix is important in deciding the suitable matrix. In the presence of soft abrasives at high stresses, wear resistance increases with an increase in carbide volume fraction [53]. Austenite is beneficial because it is ductile, strain hardens at the surface, and is metastable at high stresses such that mechanical energy is dissipated into a larger volume due to plastic deformation [8,32,44]. There is good fitting of planes between austenite matrix and carbides compared to martensite, and this may be the reason for the good wear–corrosion resistance of austenite observed in the presence of hard abrasive particles [32,45]. When handling hard abrasives at high stresses, carbides cannot protect the matrix, resulting in rapid removal of the matrix and spalling and microcracking of exposed carbides under stress; therefore, the matrix should be hard to protect carbides [154]. Thus, an increase in the volume fraction of carbides is not beneficial and compromises toughness [154]. It has been observed that steels perform better than HCWCIs under these conditions [155]. However, at moderate impacts, an austenitic matrix prevents propagation of cracks between carbides and performs better than martensite, but at excessive impacts, carbides may be broken due to excessive plastic deformation, so they will not be able to protect the matrix [66,117,156]. Some studies showed that an austenite matrix is superior to martensite under high stress and hard abrasives [32,53,155]. During the grinding of phosphate rock, it was demonstrated by Deshpande and Natarajan [157] that wear–corrosion rates are high in wet grinding compared to dry grinding. In addition, a laboratory study by Chen et al. [158] on wet grinding of phosphate rock showed that the wear–corrosion rate is very high at low pHs. Thus, grinding performed in an aqueous environment is considered to be wear–corrosive in this review regardless of the pH employed.

5.2.1. Effect of Chemical Composition

Chromium

Abrasion–corrosion research by Ribeiro et al. [159] on as-cast Fe-13Cr-2.6C and Fe-19Cr-2.8C HCWCIs using high-stress ball cratering test with hard SiC slurry showed that the alloy with higher Cr content exhibited better wear resistance due to reduced abrasive-matrix hardness difference, high matrix corrosion resistance and high macrohardness. Rajagopal and Iwasaki [160] investigated the influence of chromium addition on the corrosion behavior of HCWCIs in quartz slurry under abrasion using polarization measurements. Corrosion rates of a high Cr sample increased with an increase in abrasion intensity, while for a low Cr content sample, corrosion was high under all conditions. A high-stress ball-cratering abrasion test with large-sized silica sand and crushed quartz slurries was used by Stachowiak et al. [161] on Fe-25Cr-2.3C (hypoeutectic), Fe-27Cr-3C (hypoeutectic) and Fe-30Cr-4.5C (hypereutectic) white cast irons and an opposite wear resistance of the order 25Cr > 27Cr > 30Cr was observed in comparison with findings made in low stress slurry pumps. Higher wear resistance at lower chromium contents can be attributed to the refined morphology of the hypoeutectic alloys.

Tungsten

The influence of W on the wear–corrosion resistance of HCWCI was studied by Anijdan et al. [162]. HCWCI balls with 2.5 wt% W were heat treated to obtain a tough matrix and were used for the high-stress grinding of acidic copper ore. They demonstrated good abrasion–corrosion resistance and extended the plant's service life, but pitting was the main wear mechanism experienced.

Carbon and Nitrogen

Abrasion–corrosion testing of HCWCI and cast steel mill liners by Albright and Dunn [163] during wet grinding showed that wear–corrosion rate decreased with an increase in hardness in high C content HCWCI alloys. Computational thermodynamics was used to design high Cr matrix HCWCI balls for grinding iron ore with low chloride con-

tent [11]. Nitrogen was added to stabilize austenite; wear–corrosion rates of the designed balls were lower than those of forged steel balls, and performance was satisfactory.

5.2.2. Effect of Microstructure

Matrix

The effect of carbide volume fraction (13–41%) and different matrix microstructures on abrasion–corrosion wear behavior of HCWCI balls tested in a laboratory ball mill for 200 h was studied by Albertin and Sinatora [48,129]. In soft abrasives of hematite and phosphate rock, increasing carbide volume fraction decreased abrasion–corrosion wear rates, while in the presence of harder abrasives like quartz, the wear rate increased with an increase in carbide volume, as shown in Figure 8a. Hard martensitic microstructure performed well against quartz, while a softer pearlitic matrix was of inferior performance characterized by deformation and carbide cracking due to inhomogeneous plastic flow; these comparisons are shown in Figure 8b. At a constant carbide volume fraction of 30 wt%, laboratory ball mill tests demonstrated that the martensitic matrix was superior, followed by the austenitic and finally the pearlitic; while, on the contrary, pin-on-disc tests showed that austenitic samples were better than martensitic (due to strain hardening) when using hard SiC abrasives.

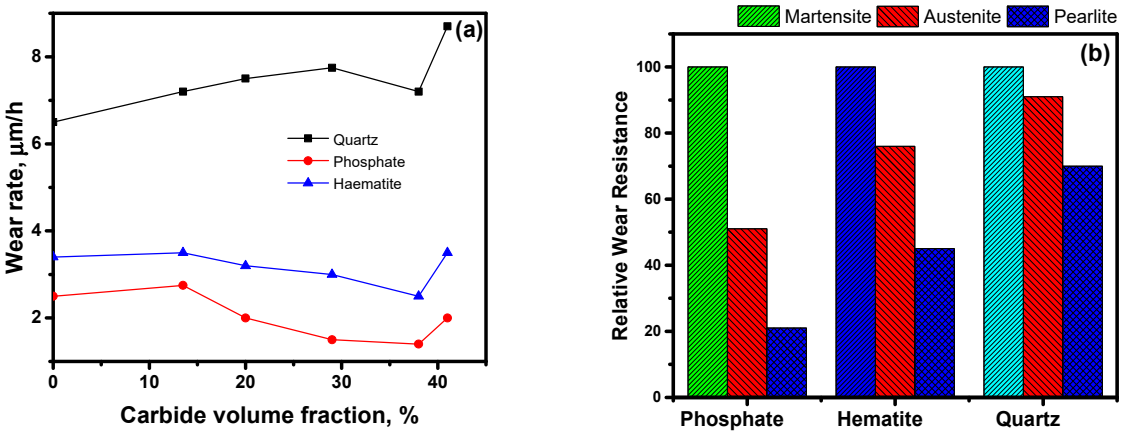


Figure 8. (**a**) The influence of carbide volume fraction on abrasion–corrosion wear rate for different abrasives; (**b**) The effect of matrix type on wear resistance during ball milling against different abrasives. Reproduced with permission [48] 2001, Elsevier.

Studies by Gates et al. [8] using a rubber wheel test showed that a Fe-15Cr-1.4C white cast iron with an austenitic matrix exhibited the best resistance to synergistic corrosion–abrasion, better than pearlitic and martensitic matrices. Abrasion–corrosion synergism in pearlitic and martensitic matrices occurred by pitting of the matrix surface followed by abrasive damage to passive films. An attack on martensite exposed carbides to attack by abrasion. In an austenitic matrix, abrasive damage of the passive film was a significant wear–corrosion mechanism, i.e., acceleration of corrosion by abrasive damage of passive films. Ball mill tests by Dodd et al. [39] showed that HCWCI with both high C and a martensitic matrix has low wear–corrosion rates in wet grinding.

Comparisons of HCWCIs with Other Materials

It was found by Chenje and Simbi [164] that HCWCIs compete with steel balls in ball milling of hard ores and that the dominant mechanism of material loss was abrasion wear. During ball milling experiments by Chenhe et al. [22,23], it was found that HCWCI balls performed better in abrasion–corrosion wear than steels. Research by Gundewar et al. [165] showed that HCWCIs have higher abrasion–corrosion resistance than forged EN31 steel and cast steel balls during wet grinding of iron ore in India. This was attributed to the passivation of HCWCIs in the presence of oxygen.

6. Future Challenges

The main challenges in the development and selection of HCWCIs for wear–corrosion environments include the following:

1. Difficulties in optimization of the chemical composition, heat treatment, and processing conditions to obtain suitable microstructures, toughness, and chemical compositions due to multiple design and fabrication variables.
2. Unavailability of wear–corrosion performance data for many HCWCIs compositions and microstructures in many environments.
3. Difficulties in evaluating performances of materials under different environments with changes in conditions (stresses, impact, and corrosivity) to establish materials wear–corrosion maps.

7. Summary

HCWCIs demonstrate different behaviors in wear–corrosion environments depending on their microstructures and chemical composition. The design, fabrication, and performance of HCWCIs in different wear–corrosion environments were reviewed, and the major findings are as follows:

1. Although HCWCIs possess excellent wear resistance, their applications in corrosive environments; for example, in ball milling of corrosive ores and pumping of acidic slurries of low pH, are still limited because of high loss rates. Appropriate alloys should have adequate hardness for wear resistance and high Cr contents in the matrix for corrosion resistance. There is a need for the development of wear–corrosion maps of HCWCIs in different environments (stresses, abrasives type and size, slurry velocity, pH, temperature) for the rapid development of appropriate alloys.
2. Several approaches were employed to improve the wear and corrosion resistance of HCWCIs. Wear resistance is mainly improved via grain refinement (using rapid solidification, low casting superheats, inoculation, and alloying), formation of strong carbides using alloying, formation of desired microstructure during casting and heat treatment, and appropriate heat treatment to precipitate carbides. Corrosion resistance is improved via enhancing Cr content in the matrix using strong carbide formers to consume C, formation of appropriate microstructures during solidification, and optimum destabilization heat treatment temperature to dissolve carbides.
3. Application of computational modeling to guide chemical composition, casting, and heat treatment design rather than trial and error for fast development of HCWCIs is gaining acceptance amongst researchers. Approaches like computational thermodynamics and artificial neural network modeling may provide guidance on important parameters and properties since multiple variables are involved, from alloy fabrication to industrial testing.
4. Wear rate depends on the hardness of abrasives and severity of loading. Austenitic and martensitic matrices are usually considered in wear–corrosion environments. Austenitic matrices are more applicable in wear–corrosion environments with strain hardening since they contain high Cr contents and are tough. They are most suitable for severe erosion–corrosion conditions, even at high abrasive impingement angles. The carbide content should be reduced to enhance toughness, and carbide interspacing should be smaller than the eroding particles. Martensitic microstructures are applicable in conditions where austenite cannot strain harden since they are hard and brittle, but they should be saturated with high contents of Cr for corrosion resistance. Typical applications include high-stress abrasive sliding with low impacts, like neutral ore grinding.
5. Abrasives should be carefully selected, and moderate conditions can properly demonstrate differences in performances. The use of much harder abrasives like quartz, SiC, and alumina tends to compress materials' performance because of rapid wear such that performance differences are not clearly distinguished. An increase in carbide volume fraction decreases wear rate either at low stress or when handling softer abrasives

at high stresses, and for harder abrasives at high stress, the type of microstructure is important and should be hard. Many results on the design and performance of HCWCIs are still at the laboratory scale and should be upgraded to the field scale.

Author Contributions: Conceptualization, S.F. and V.T.; writing—original draft preparation, S.F.; writing—review and editing, S.F. and V.T.; supervision, V.T. All authors have read and agreed to the published version of the manuscript.

Funding: This research received no external funding.

Data Availability Statement: Data sharing is not applicable. No new data were created or analyzed in this study. Data sharing is not applicable to this article.

Acknowledgments: The authors would like to thank the OCP Foundation for its financial support.

Conflicts of Interest: The authors declare no conflict of interest.

References

1. Puspasari, V.; Herbirowo, S.; Habieb, A.M.; Utama, D.P.; Roberto, R.; Adjiantoro, B. Effect of sub-zero treatments on hardness and corrosion properties of low-alloy nickel steel. *AIMS Mater. Sci.* **2023**, *10*, 55–69. [CrossRef]
2. Gangopadhyay, A.K.; Moore, J.J. The role of abrasion and corrosion in grinding media wear. *Wear* **1985**, *104*, 49–64. [CrossRef]
3. Iwasaki, I.; Riemer, S.C.; Orlich, J.N.; Natarajan, K.A. Corrosive and abrasive wear in ore grinding. *Wear* **1985**, *103*, 253–267. [CrossRef]
4. Jones, D.A. Corrosive wear in wet ore grinding systems. *JOM* **1985**, *37*, 20–23. [CrossRef]
5. Chelgani, S.C.; Parian, M.; Parapari, P.S.; Ghorbani, Y.; Rosenkranz, J. A comparative study on the effects of dry and wet grinding on mineral flotation separation–a review. *J. Mater. Res. Technol.* **2019**, *8*, 5004–5011. [CrossRef]
6. Gates, J.D.; Dargusch, M.S.; Walsh, J.J.; Field, S.L.; Hermand, M.-P.; Delaup, B.G.; Saad, J.R. Effect of abrasive mineral on alloy performance in the ball mill abrasion test. *Wear* **2008**, *265*, 865–870. [CrossRef]
7. Zheng, Y.; Yao, Z.; Wei, X.; Ke, W. The synergistic effect between erosion and corrosion in acidic slurry medium. *Wear* **1995**, *186*, 555–561. [CrossRef]
8. Gates, J.D.; Lai, W.Q.; Wen, P.S.; Hope, G.A.; Holt, S.A. Synergistic corrosion-abrasion of cast wear-resistant materials in HNO_3. *Cast Met.* **1995**, *8*, 73–90. [CrossRef]
9. Soleymani, M.M.; Bahiraie, M.; Rezaeizadeh, M. Investigating the contribution of wear caused by impact and abrasion in semi autogenous grinding mills. *Int. J. Iron Steel Soc. Iran.* **2022**, *19*, 59–65.
10. Efremenko, V.G.; Shimizu, K.; Noguchi, T.; Efremenko, A.V.; Chabak, Y.G. Impact–abrasive–corrosion wear of Fe-based alloys: Influence of microstructure and chemical composition upon wear resistance. *Wear* **2013**, *305*, 155–165. [CrossRef]
11. Albertin, E.; Beneduce, F.; Matsumoto, M.; Teixeira, I. Optimizing heat treatment and wear resistance of high chromium cast irons using computational thermodynamics. *Wear* **2011**, *271*, 1813–1818. [CrossRef]
12. Gonzalez-Pociño, A.; Alvarez-Antolin, F.; Asensio-Lozano, J. Optimization of thermal processes applied to hypoeutectic white cast iron containing 25% Cr aimed at increasing erosive wear resistance. *Metals* **2020**, *10*, 359. [CrossRef]
13. Aldrich, C. Consumption of steel grinding media in mills–A review. *Miner. Eng.* **2013**, *49*, 77–91. [CrossRef]
14. Wang, Z.; Yang, Y.; Chen, C.; Li, Y.; Yang, Z.; Lv, B.; Zhang, F. Effect of Surface Impacting Parameters on Wear Resistance of High Manganese Steel. *Coatings* **2023**, *13*, 539. [CrossRef]
15. Liu, Y.; Sun, J.-B.; Liu, S.-J.; Liu, Z.; Yin, F.-X. Optimization of Ultra-High and High Manganese Steel Based on Artificial Neural Network and Genetic Algorithm. *J. Mater. Eng. Perform.* **2023**, *32*, 9864–9874. [CrossRef]
16. Zellagui, R.; Hemmouche, L.; Bouchafaa, H.; Belrechid, R.; Aitsadi, H.; Chelli, A.; Touil, M.; Djalleb, N. Effect of heat treatments on the microstructure, mechanical, wear and corrosion resistance of casted hadfield steel. *Int. J. Met.* **2022**, *16*, 2050–2064. [CrossRef]
17. Sezgin, C.T.; Hayat, F. The effects of boriding process on tribological properties and corrosive behavior of a novel high manganese steel. *J. Mater. Process. Technol.* **2022**, *300*, 117421. [CrossRef]
18. Sudhakar, A.N.; Markandeya, R.; Ajoy, K.P.; Kaushik, D. Effect of alloying elements on the microstructure and mechanical properties of high chromium white cast iron and Ni-Hard iron. *Mater. Today Proc.* **2022**, *61*, 1006–1014.
19. Karafyllias, G.; Galloway, A.; Humphries, E. The effect of low pH in erosion-corrosion resistance of high chromium cast irons and stainless steels. *Wear* **2019**, *420*, 79–86. [CrossRef]
20. Karafyllias, G.; Galloway, A.; Humphries, E. Erosion-corrosion assessment in strong acidic conditions for a white cast iron and UNS S31600 stainless steel. *Wear* **2021**, *484*, 203665. [CrossRef]
21. Jokari-Sheshdeh, M.; Ali, Y.; Gallo, S.C.; Lin, W.; Gates, J.D. Comparing the abrasion performance of NiHard-4 and high-Cr-Mo white cast irons: The effects of chemical composition and microstructure. *Wear* **2022**, *492*, 204208. [CrossRef]
22. Chenje, T.W.; Simbi, D.J.; Navara, E. Relationship between microstructure, hardness, impact toughness and wear performance of selected grinding media for mineral ore milling operations. *Mater. Des.* **2004**, *25*, 11–18. [CrossRef]

23. Chenje, T.W.; Simbi, D.J.; Navara, E. The role of corrosive wear during laboratory milling. *Miner. Eng.* **2003**, *16*, 619–624. [CrossRef]
24. Nodir, T.; Nosir, S.; Shirinkhon, T.; Erkin, K.; Azizakhon, T.; Mukhammadali, A. Development Of Technology To Increase Resistance Of High Chromium Cast Iron. *Am. J. Eng. Technol.* **2021**, *3*, 85–92.
25. Zhu, Y.; Liu, H.; Wang, J.; Yan, F. Antagonistic effect of electrochemical corrosion on the mechanical wear of Monel 400 alloy in seawater. *Corros. Sci.* **2022**, *198*, 110120. [CrossRef]
26. Zheng, Z.; Long, J.; Guo, Y.; Li, H.; Zheng, K.; Qiao, Y. Corrosion and impact–abrasion–corrosion behaviors of quenching–tempering martensitic Fe–Cr alloy steels. *J. Iron Steel Res. Int.* **2022**, *29*, 1853–1863. [CrossRef]
27. Chintha, A.R. Metallurgical aspects of steels designed to resist abrasion, and impact-abrasion wear. *Mater. Sci. Technol.* **2019**, *35*, 1133–1148. [CrossRef]
28. Ba, L.; Gao, Q.; Cen, W.; Wang, J.; Wen, Z. The impact-abrasive wear behavior of high wear resistance filling pipeline with explosion treatment. *Vacuum* **2021**, *192*, 110427. [CrossRef]
29. Batchelor, A.W.; Stachowiak, G.W. Predicting synergism between corrosion and abrasive wear. *Wear* **1988**, *123*, 281–291. [CrossRef]
30. Massola, C.P.; Chaves, A.P.; Albertin, E. A discussion on the measurement of grinding media wear. *J. Mater. Res. Technol.* **2016**, *5*, 282–288. [CrossRef]
31. Islam, M.A.; Farhat, Z. Erosion-corrosion mechanism and comparison of erosion-corrosion performance of API steels. *Wear* **2017**, *376*, 533–541. [CrossRef]
32. Tabrett, C.P.; Sare, I.R.; Ghomashchi, M.R. Microstructure-property relationships in high chromium white iron alloys. *Int. Mater. Rev.* **1996**, *41*, 59–82. [CrossRef]
33. Tang, X.H.; Chung, R.; Pang, C.J.; Li, D.Y.; Hinckley, B.; Dolman, K. Microstructure of high (45 wt.%) chromium cast irons and their resistances to wear and corrosion. *Wear* **2011**, *271*, 1426–1431. [CrossRef]
34. Pourasiabi, H.; Gates, J.D. Effects of niobium macro-additions to high chromium white cast iron on microstructure, hardness and abrasive wear behaviour. *Mater. Des.* **2021**, *212*, 110261. [CrossRef]
35. Huang, G.; Grano, S. Galvanic interaction between grinding media and arsenopyrite and its effect on flotation: Part I. Quantifying galvanic interaction during grinding. *Int. J. Miner. Process.* **2006**, *78*, 182–197. [CrossRef]
36. Jankovic, A.; Wills, T.; Dikmen, S. A comparison of wear rates of ball mill grinding media. *J. Min. Metall. A Min.* **2016**, *52*, 1–10. [CrossRef]
37. Huq, M.J.; Shimizu, K.; Kusumoto, K.; Purba, R.H. Three-body abrasive wear performance of high chromium white cast iron with different Ti and C content. *Lubricants* **2022**, *10*, 348. [CrossRef]
38. Azizi, A.; Shafaei, S.Z.; Noaparast, M.; Karamoozian, M. An investigation of the corrosive wear of steel balls in grinding of sulphide ores. *Int. J. Min. Geo-Eng.* **2015**, *49*, 83–91.
39. Dodd, J.; Dunn, D.J.; Huiatt, J.L.; Norman, T.E. Relative importance of abrasion and corrosion in metal loss in ball milling. *Min. Metall. Explor.* **1985**, *2*, 212–216. [CrossRef]
40. Shah, M.; Sahoo, K.L.; Das, S.K.; Das, G. Wear mechanism of high chromium white cast iron and its microstructural evolutions during the comminution process. *Tribol. Lett.* **2020**, *68*, 77. [CrossRef]
41. Pintaude, G.; Albertin, E.; Sinatora, A. A review on abrasive wear mechanisms of metallic materials. In *Proceedings of the International Conference on Abrasion Wear Resistant Alloyed White Cast Iron for Rolling and Pulverizing Mills*; IPT/EPUSP: Sao Paulo, Brazil, 2005.
42. Iwasaki, I.; Pozzo, R.L.; Natarajan, K.A.; Adam, K.; Orlich, J.N. Nature of corrosive and abrasive wear in ball mill grinding. *Int. J. Miner. Process.* **1988**, *22*, 345–360. [CrossRef]
43. Rao, M.K.Y.; Natarajan, K.A. Factors influencing ball wear and flotation with respect to ore grinding. *Miner. Procesing Extr. Metall. Rev.* **1991**, *7*, 137–173.
44. Doğan, Ö.N.; Hawk, J.A.; Laird, G. Solidification structure and abrasion resistance of high chromium white irons. *Metall. Mater. Trans. A* **1997**, *28*, 1315–1328. [CrossRef]
45. Jain, A.-S.; Chang, H.; Tang, X.; Hinckley, B.; Zhang, M.-X. Refinement of primary carbides in hypereutectic high-chromium cast irons: A review. *J. Mater. Sci.* **2021**, *56*, 999–1038. [CrossRef]
46. Ibrahim, M.M.; El-Hadad, S.; Mourad, M. Enhancement of wear resistance and impact toughness of as cast hypoeutectic high chromium cast iron using niobium. *Int. J. Cast Met. Res.* **2018**, *31*, 72–79. [CrossRef]
47. Powell, G.L.F.; Laird, G. Structure, nucleation, growth and morphology of secondary carbides in high chromium and Cr-Ni white cast irons. *J. Mater. Sci.* **1992**, *27*, 29–35. [CrossRef]
48. Albertin, E.; Sinatora, A. Effect of carbide fraction and matrix microstructure on the wear of cast iron balls tested in a laboratory ball mill. *Wear* **2001**, *250*, 492–501. [CrossRef]
49. Kopyciński, D.; Piasny, S. Influence of tungsten and titanium on the structure of chromium cast iron. *Arch. Foundry Eng.* **2012**, *12*, 57–60. [CrossRef]
50. Tang, X.H.; Chung, R.; Li, D.Y.; Hinckley, B.; Dolman, K. Variations in microstructure of high chromium cast irons and resultant changes in resistance to wear, corrosion and corrosive wear. *Wear* **2009**, *267*, 116–121. [CrossRef]
51. Zumelzu, E.; Goyos, I.; Cabezas, C.; Opitz, O.; Parada, A. Wear and corrosion behaviour of high-chromium (14–30% Cr) cast iron alloys. *J. Mater. Process. Technol.* **2002**, *128*, 250–255. [CrossRef]
52. Maratray, F. Choice of appropriate compositions for chromium-molybdenum white irons. *AFS Trans.* **1971**, *79*, 121–124.

53. Gahr, K.-H.Z.; Doane, D.V. Optimizing fracture toughness and abrasion resistance in white cast irons. *Metall. Trans. A* **1980**, *11*, 613–620. [CrossRef]
54. Do, Ö.N.; Hawk, J.A. Effect of carbide orientation on abrasion of high Cr white cast iron. *Wear* **1995**, *189*, 136–142.
55. Dogan, O.N. Columnar to equiaxed transition in high Cr white iron castings. *Scr. Mater.* **1996**, *35*, 163–168. [CrossRef]
56. Karantzalis, E.; Lekatou, A.; Mavros, H. Microstructure and properties of high chromium cast irons: Effect of heat treatments and alloying additions. *Int. J. Cast Met. Res.* **2009**, *22*, 448–456. [CrossRef]
57. Lu, B.; Luo, J.; Chiovelli, S. Corrosion and wear resistance of chrome white irons—A correlation to their composition and microstructure. *Metall. Mater. Trans. A* **2006**, *37*, 3029–3038. [CrossRef]
58. Kahar, S.D. Duplex stainless steels-an overview. *Int. J. Eng. Res. Appl.* **2017**, *7*, 27–36. [CrossRef]
59. Painkra, T.K.; Naik, K.S.; Nishad, R.K.; Sen, P.K.; Bohidar, S.K. Review about high performance of Austenitic Stainless Steel. *Int. J. Innov. Res. Sci. Technol.* **2014**, *1*, 93–99.
60. Adler, T.A.; Doğan, Ö.N. Erosive wear and impact damage of high-chromium white cast irons. *Wear* **1999**, *225*, 174–180. [CrossRef]
61. Zhang, A.F.; Xing, J.D.; Fang, L.; Su, J.Y. Inter-phase corrosion of chromium white cast irons in dynamic state. *Wear* **2004**, *257*, 198–204. [CrossRef]
62. Zhang, T.; Li, D.Y. Modification of 27Cr cast iron with alloying yttrium for enhanced resistance to sliding wear in corrosive media. *Metall. Mater. Trans. A* **2002**, *33*, 1981–1989. [CrossRef]
63. Chung, R.J.; Tang, X.; Li, D.Y.; Hinckley, B.; Dolman, K. Microstructure refinement of hypereutectic high Cr cast irons using hard carbide-forming elements for improved wear resistance. *Wear* **2013**, *301*, 695–706. [CrossRef]
64. Kootsookos, A.; Gates, J.D.; Eaton, R.A. Development of a white cast iron of fracture toughness 40 MPa$\sqrt{}$m. *Cast Met.* **1995**, *7*, 239–246. [CrossRef]
65. Hua-Qin, S.; Chongxi, T.; Xu-Ru, Y.; Qigui, W. Study on Raising the Impact Toughness of Wear-Resistant High--Chromium Cast Iron. In Proceedings of the Ninety-Fifth Annual Meeting American Foundrymen's Society, Milwaukee, WI, USA, August 1991; pp. 333–337.
66. Pearce, J.T.H. Structure and Wear Performance of Abrasion Resistant Chromium White Cast Irons. (Retroactive Coverage). *Trans. Am. Foundrymen's Soc.* **1984**, *92*, 599–622.
67. Liu, S.; Wang, Z.; Shi, Z.; Zhou, Y.; Yang, Q. Experiments and calculations on refining mechanism of NbC on primary M_7C_3 carbide in hypereutectic Fe-Cr-C alloy. *J. Alloys Compd.* **2017**, *713*, 108–118. [CrossRef]
68. Pourasiabi, H.; Gates, J.D. Effects of chromium carbide volume fraction on high-stress abrasion performance of NbC-bearing high chromium white cast irons. *Wear* **2022**, *498*, 204312. [CrossRef]
69. Bedolla-Jacuinde, A.; Guerra, F.V.; Mejía, I.; Zuno-Silva, J.; Rainforth, M. Abrasive wear of V–Nb–Ti alloyed high-chromium white irons. *Wear* **2015**, *332*, 1006–1011. [CrossRef]
70. Sharma, D.K.; Mahant, D.; Upadhyay, G. Manufacturing of metal matrix composites: A state of review. *Mater. Today Proc.* **2020**, *26*, 506–519. [CrossRef]
71. Stefanescu, D.M. Solidification of metal matrix composites. In *Science and Engineering of Casting Solidification*; Springer: Cham, Switzerland, 2015; pp. 305–341.
72. Ohno, M. Quantitative phase-field modeling and simulations of solidification microstructures. *ISIJ Int.* **2020**, *60*, 2745–2754. [CrossRef]
73. Tourret, D.; Liu, H.; LLorca, J. Phase-field modeling of microstructure evolution: Recent applications, perspectives and challenges. *Prog. Mater. Sci.* **2022**, *123*, 100810. [CrossRef]
74. Filipovic, M.; Kamberovic, Z.; Korac, M.; Jordovic, B. Effect of niobium and vanadium additions on the as-cast microstructure and properties of hypoeutectic Fe–Cr–C alloy. *ISIJ Int.* **2013**, *53*, 2160–2166. [CrossRef]
75. Fiset, M.; Peev, K.; Radulovic, M. The influence of niobium on fracture toughness and abrasion resistance in high-chromium white cast irons. *J. Mater. Sci. Lett.* **1993**, *12*, 615–617. [CrossRef]
76. Sarac, M.F.; Dikici, B. Effect of heat treatment on wear and corrosion behavior of high chromium white cast iron. *Mater. Test.* **2019**, *61*, 659–666. [CrossRef]
77. Tabrett, C.P.; Sare, I.R. The effect of heat treatment on the abrasion resistance of alloy white irons. *Wear* **1997**, *203*, 206–219. [CrossRef]
78. Zhi, X.; Xing, J.; Fu, H.; Xiao, B. Effect of niobium on the as-cast microstructure of hypereutectic high chromium cast iron. *Mater. Lett.* **2008**, *62*, 857–860. [CrossRef]
79. Nayak, U.P.; Guitar, M.A.; Mücklich, F. A comparative study on the influence of chromium on the phase fraction and elemental distribution in as-cast high chromium cast irons: Simulation vs. experimentation. *Metals* **2020**, *10*, 30. [CrossRef]
80. Yamamoto, K.; Inthidech, S.; Sasaguri, N.; Matsubara, Y. Influence of Mo and W on high temperature hardness of M_7C_3 carbide in high chromium white cast iron. *Mater. Trans.* **2014**, *55*, 684–689. [CrossRef]
81. Lv, Y.; Sun, Y.; Zhao, J.; Yu, G.; Shen, J.; Hu, S. Effect of tungsten on microstructure and properties of high chromium cast iron. *Mater. Des.* **2012**, *39*, 303–308. [CrossRef]
82. Sanchez-Cruz, A.; Bedolla-Jacuinde, A.; Guerra, F.V.; Mejía, I. Microstructural modification of a static and dynamically solidified high chromium white cast iron alloyed with vanadium. *Results Mater.* **2020**, *7*, 100114. [CrossRef]
83. Mampuru, L.A.; Maruma, M.G.; Moema, J.S. Grain refinement of 25 wt% high-chromium white cast iron by addition of vanadium. *J. S. Afr. Inst. Min. Metall.* **2016**, *116*, 969–972. [CrossRef]

84. Mohammadnezhad, M.; Javaheri, V.; Shamanian, M.; Naseri, M.; Bahrami, M. Effects of vanadium addition on microstructure, mechanical properties and wear resistance of Ni-Hard4 white cast iron. *Mater. Des.* **2013**, *49*, 888–893. [CrossRef]
85. Zhao, W.M.; Liu, Z.X.; Ju, Z.L.; Liao, B.; Chen, X.G. Effects of vanadium and rare-earth on carbides and properties of high chromium cast iron. In *Materials Science Forum*; Trans Tech Publications Ltd.: Bäch, Switzerland, 2008; pp. 1414–1419.
86. Aso, S.; Goto, S.; Komatsu, Y.; Liu, W.; Liu, C. The effect of solidification conditions on phase transformation of iron matrix of Fe-25mass% Cr-CB alloys. *Int. J. Cast Met. Res.* **1999**, *11*, 285–290. [CrossRef]
87. Xu, L.; Wang, F.; Lu, F.; Zhou, Y.; Chen, C.; Wei, S. Microstructure and erosion wear properties of high chromium cast iron added nitrogen by high pressure in alkaline sand slurry. *Wear* **2021**, *476*, 203655. [CrossRef]
88. Lu, F.; Wei, S.; Xu, L.; Zhou, Y.; Wang, X.; Wang, F.; Yi, X. Erosion–wear behaviors of high-chromium cast iron with high nitrogen content in water–sand slurry and acid–sand slurry. *Tribol. Trans.* **2020**, *63*, 325–335. [CrossRef]
89. Ding, H.; Liu, S.; Zhang, H.; Guo, J. Improving impact toughness of a high chromium cast iron regarding joint additive of nitrogen and titanium. *Mater. Des.* **2016**, *90*, 958–968. [CrossRef]
90. Göcmen, A.; Ernst, P.; Holmes, P. Principles of alloy design in high nitrogen 12% chromium steels. In *Materials Science Forum*; Trans Tech Publications Ltd.: Bäch, Switzerland, 1999; pp. 215–226.
91. Xu, L.; Wang, F.; Li, M.; Li, F.; Wang, X.; Jiang, T.; Deng, X.; Wei, S. Fabrication and abrasive wear property of high chromium cast iron with high vanadium and high nitrogen content (HCCI-VN). *Wear* **2023**, *523*, 204828. [CrossRef]
92. Tabrett, C.P.; Sare, I.R. Effect of high temperature and sub-ambient treatments on the matrix structure and abrasion resistance of a high-chromium white iron. *Scr. Mater.* **1998**, *38*, 1747–1753. [CrossRef]
93. Agakhanov, E.K.; Agakhanov, M.K.; Agakhanova, R.E. Stress modelling in natural foundation. In *IOP Conference Series: Materials Science and Engineering*; IOP Publishing: Bristol, UK, 2020; Volume 1001, p. 012072.
94. Li, Y.; Yan, S.; Zhang, J.; Zhu, X. Deformation behaviour of high chromium cast iron/low-carbon steel laminates based on hot rolling and finite element simulation. *Vacuum* **2023**, *214*, 112218. [CrossRef]
95. Chung, R.J.; Tang, X.; Li, D.Y.; Hinckley, B.; Dolman, K. Abnormal erosion–slurry velocity relationship of high chromium cast iron with high carbon concentrations. *Wear* **2011**, *271*, 1454–1461. [CrossRef]
96. Llewellyn, R.J.; Yick, S.K.; Dolman, K.F. Scouring erosion resistance of metallic materials used in slurry pump service. *Wear* **2004**, *256*, 592–599. [CrossRef]
97. Eiselstein, L.E.; Ruano, O.A.; Sherby, O.D. Structural characterization of rapidly solidified white cast iron powders. *J. Mater. Sci.* **1983**, *18*, 483–492. [CrossRef]
98. Seah, K.H.W.; Hemanth, J.; Sharma, S.C. Wear characteristics of sub-zero chilled cast iron. *Wear* **1996**, *192*, 134–140. [CrossRef]
99. Liu, Q.; Zhang, H.; Wang, Q.; Zhou, X.; Jönsson, P.G.; Nakajima, K. Effect of cooling rate and Ti addition on the microstructure and mechanical properties in as-cast condition of hypereutectic high chromium cast irons. *ISIJ Int.* **2012**, *52*, 2210–2219. [CrossRef]
100. Yang, D.-S.; Lei, T.-S. Investigating the influence of mid-chilling on microstructural development of high-chromium cast iron. *Mater. Manuf. Process.* **2012**, *27*, 919–924. [CrossRef]
101. Laird, G.; Doğan, Ö.N. Solidification structure versus hardness and impact toughness in high-chromium white cast irons. *Int. J. Cast Met. Res.* **1996**, *9*, 83–102. [CrossRef]
102. Huang, Z. Investigation of microstructure and impact toughness of semisolid hypereutectic high chromium cast iron prepared by slope cooling body method. *J. Appl. Sci.* **2006**, *6*, 1635–1640. [CrossRef]
103. Zhi, X.; Liu, J.; Xing, J.; Ma, S. Effect of cerium modification on microstructure and properties of hypereutectic high chromium cast iron. *Mater. Sci. Eng. A* **2014**, *603*, 98–103. [CrossRef]
104. Qu, Y.; Xing, J.; Zhi, X.; Peng, J.; Fu, H. Effect of cerium on the as-cast microstructure of a hypereutectic high chromium cast iron. *Mater. Lett.* **2008**, *62*, 3024–3027. [CrossRef]
105. Dojka, M.; Dojka, R. Inhibition of Carbide Growth by Sr in High-Alloyed White Cast Iron. *Materials* **2022**, *15*, 1317. [CrossRef]
106. Fu, H.; Wu, X.; Li, X.; Xing, J.; Lei, Y.; Zhi, X. Effect of TiC particle additions on structure and properties of hypereutectic high chromium cast iron. *J. Mater. Eng. Perform.* **2009**, *18*, 1109–1115. [CrossRef]
107. Guzik, E.; Kopyciński, D.; Burbelko, A.; Szczęsny, A. Evaluation of the number of primary grains in hypoeutectic chromium cast iron with different wall thickness using the ProCAST program. *Materials* **2023**, *16*, 3217. [CrossRef] [PubMed]
108. Kopyciński, D. Inoculation of chromium white cast iron. *Arch. Foundry Eng.* **2009**, *9*, 191–194.
109. Feifei, H.; Bo, L.; Da, L.; Ting, D.A.N.; Xuejun, R.E.N.; Qingxiang, Y.; Ligang, L.I.U. Effects of rare earth oxide on hardfacing metal microstructure of medium carbon steel and its refinement mechanism. *J. Rare Earths* **2011**, *29*, 609–613.
110. Feifei, H.; Da, L.; Ting, D.; Xuejun, R.E.N.; Bo, L.; Qingxiang, Y. Effect of rare earth oxides on the morphology of carbides in hardfacing metal of high chromium cast iron. *J. Rare Earths* **2011**, *29*, 168–172.
111. Gittus, J.H. Inoculation of solidifying iron and steel casting by means of vibration. *J. Iron Steel Inst.* **1959**, *192*, 118–131.
112. Nofal, A.; Reda, R.; Ibrahim, K.M.; Hussein, A. Structural refinement of 15% Cr-2% Mo white irons. *Key Eng. Mater.* **2011**, *457*, 231–236. [CrossRef]
113. Kocatepe, K.; Burdett, C.F. Effect of low frequency vibration on macro and micro structures of LM6 alloys. *J. Mater. Sci.* **2000**, *35*, 3327–3335. [CrossRef]
114. Appendino, P.; Crivellone, G.; Mus, C.; Spriano, S. Dynamic solidification of sand-cast aluminium alloys. *Metall. Sci. Tecnol.* **2002**, *20*, 27–32.

115. Zhou, R.F.; Jiang, Y.H.; Zhou, R.; Zhang, L. Effect of Electric Current Pulse on Solidification Microstructure of Hypereutectic high Chromium CAST iron Cooling from the Temperature between Liquidus and Solidus. 2014. 10th International Symposium on the Science and Processing of Cast Iron. 2014. Argentina: Mar del Plata 10 to 13th of November. Available online: http://rinfi.fi.mdp.edu.ar/xmlui/handle/123456789/23 (accessed on 29 September 2023).
116. Chen, H.; Zhou, R.F.; Jiang, Y.H.; Zhou, R. Effect of electric current pulse on carbide in hypereutectic high chromium cast iron. *Adv. Mater. Res.* **2012**, *457*, 174–180. [CrossRef]
117. Penagos, J.J.; Pereira, J.I.; Machado, P.C.; Albertin, E.; Sinatora, A. Synergetic effect of niobium and molybdenum on abrasion resistance of high chromium cast irons. *Wear* **2017**, *376*, 983–992. [CrossRef]
118. Girelli, L.; Pola, A.; Gelfi, M.; Masotti, M.N.; La Vecchia, G.M. Performance optimization of high resistant white cast iron for severe working applications. *Met. Ital.* **2017**, *109*, 5–10.
119. Sare, I.R.; Arnold, B.K.; Dunlop, G.A.; Lloyd, P.G. Repeated impact-abrasion testing of alloy white cast irons. *Wear* **1993**, *162*, 790–801. [CrossRef]
120. Jia, X.; Hao, Q.; Zuo, X.; Chen, N.; Rong, Y. High hardness and toughness of white cast iron: The proposal of a novel process. *Mater. Sci. Eng. A* **2014**, *618*, 96–103. [CrossRef]
121. Inthidech, S.; Sricharoenchai, P.; Matsubara, Y. Effect of molybdenum content on subcritical heat treatment behaviour of hypoeutectic 16 and 26 wt-% chromium cast irons. *Int. J. Cast Met. Res.* **2012**, *25*, 257–263. [CrossRef]
122. Opapaiboon, J.; Ayudhaya, M.S.N.; Sricharoenchai, P.; Inthidech, S.; Matsubara, Y. Effect of chromium content on heat treatment behavior of multi-alloyed white cast iron for abrasive wear resistance. *Mater. Trans.* **2019**, *60*, 346–354. [CrossRef]
123. Liu, X.; Xu, P.; Zhao, J.; Lu, W.; Li, M.; Wang, G. Material machine learning for alloys: Applications, challenges and perspectives. *J. Alloys Compd.* **2022**, *921*, 165984. [CrossRef]
124. Hart, G.L.W.; Mueller, T.; Toher, C.; Curtarolo, S. Machine learning for alloys. *Nat. Rev. Mater.* **2021**, *6*, 730–755. [CrossRef]
125. Yen, C.-L.; Liu, K.-L.; Pan, Y.-N. Simulation of the phase diagrams for high chromium white cast irons and multi-component white cast irons. *Adv. Mater. Res.* **2014**, *848*, 39–45. [CrossRef]
126. Akyildiz, Ö.; Candemir, D.; Yildirim, H. Simulation of phase equilibria in high chromium white cast irons. *Uludağ Univ. J. Fac. Eng.* **2018**, *23*, 3.
127. Jain, A.-S.; Chang, H.; Ahmad, H.; Ma, X.; Zhang, M.-X. Effect of solutes on the formation of primary carbides during solidification of hypereutectic high chromium cast irons through thermodynamic modeling. *J. Mater. Sci.* **2022**, *57*, 1429–14447. [CrossRef]
128. Wang, K.; Li, D. Formation of core (M_7C_3)-shell ($M_{23}C_6$) structured carbides in white cast irons: A thermo-kinetic analysis. *Comput. Mater. Sci.* **2018**, *154*, 111–121. [CrossRef]
129. Albertin, E.; Sinatora, A.; Pintaúde, G.; Parada, A. Study on the Performance of High Chromium Cast Iron Balls With Varied Carbide Fractions And Matrix Microstructures. ABRASION 2002. In Proceedings of the International Congress on Abrasion Wear Resistant Alloyed White Cast Iron for Rolling and Pulverizing Mills, Fukuoka, Japan, 16–20 August 2002; Volume 1. [CrossRef]
130. Tomlinson, W.J.; Talks, M.G. Erosion and corrosion of pure iron under cavitating conditions. *Ultrasonics* **1991**, *29*, 171–175. [CrossRef]
131. Kwok, C.T.; Cheng, F.T.; Man, H.C. Synergistic effect of cavitation erosion and corrosion of various engineering alloys in 3.5% NaCl solution. *Mater. Sci. Eng. A* **2000**, *290*, 145–154. [CrossRef]
132. Al-Bukhaiti, M.A.; Ahmed, S.M.; Badran, F.M.F.; Emara, K.M. Effect of impingement angle on slurry erosion behaviour and mechanisms of 1017 steel and high-chromium white cast iron. *Wear* **2007**, *262*, 1187–1198. [CrossRef]
133. Yoganandh, J.; Natarajan, S.; Babu, S.P.K. Erosive wear behavior of high-alloy cast iron and duplex stainless steel under mining conditions. *J. Mater. Eng. Perform.* **2015**, *24*, 3588–3598. [CrossRef]
134. Tian, H.H.; Addie, G.R. Experimental study on erosive wear of some metallic materials using Coriolis wear testing approach. *Wear* **2005**, *258*, 458–469. [CrossRef]
135. Tian, H.H.; Addie, G.R.; Visintainer, R.J. Erosion–corrosion performance of high-Cr cast iron alloys in flowing liquid–solid slurries. *Wear* **2009**, *267*, 2039–2047. [CrossRef]
136. Islam, A.; Jiang, J.J.; Xie, Y. Erosion-Corrosion Performance Evaluation of Different Materials for Oil Sand Application. In Proceedings of the AMPP Annual Conference + Expo, OnePetro, San Antonio, TX, USA, 6 March 2022.
137. Islam, A.; Jiang, J.J.; Xie, Y. Erosion-Corrosion Assessment of CR White Irons. In *NACE CORROSION*; OnePetro: San Antonio, TX, USA, 2021.
138. Salasi, M.; Stachowiak, G.B.; Stachowiak, G.W. Three-body tribocorrosion of high-chromium cast irons in neutral and alkaline environments. *Wear* **2011**, *271*, 1385–1396. [CrossRef]
139. Imurai, S.; Thanachayanont, C.; Pearce, J.T.H.; Chairuangsri, T. Microstructure and erosion-corrosion behaviour of as-cast high chromium white irons containing molybdenum in aqueous sulfuric-acid slurry. *Arch. Metall. Mater.* **2015**, *60*, 919–923. [CrossRef]
140. Wang, M.-C.; Ren, S.-Z.; Wang, X.-B.; Li, S.-Z. A study of sand slurry erosion of W-alloy white cast irons. *Wear* **1993**, *160*, 259–264. [CrossRef]
141. Zhang, T.; Li, D.Y. Effect of alloying yttrium on corrosion–erosion behavior of 27Cr cast white iron in different corrosive slurries. *Mater. Sci. Eng. A* **2002**, *325*, 87–97. [CrossRef]
142. Radulovic, M.; Fiset, M.; Peev, K. Effect of rare earth elements on microstructure and properties of high chromium white iron. *Mater. Sci. Technol.* **1994**, *10*, 1057–1062. [CrossRef]

143. Lu, H.; Li, T.; Cui, J.; Li, Q.; Li, D.Y. Improvement in erosion-corrosion resistance of high-chromium cast irons by trace boron. *Wear* **2017**, *376*, 578–586. [CrossRef]
144. Naiheng, M.A.; Qichang, R.; Qingde, Z. Corrosion-abrasion wear resistance of 28% Cr white cast iron containing boron. *Wear* **1989**, *132*, 347–359. [CrossRef]
145. Giourntas, L.; Brownlie, F.; Hodgkiess, T.; Galloway, A.M. Influence of metallic matrix on erosion-corrosion behaviour of high chromium cast irons under slurry impingement conditions. *Wear* **2021**, *477*, 203834. [CrossRef]
146. Karafyllias, G.; Giourntas, L.; Galloway, A.; Hodgkiess, T. Relative Performance of Two Cast Irons and Two Stainless Steels under Erosion-Corrosion Conditions. In *NACE CORROSION*; OnePetro: San Antonio, TX, USA, 2016.
147. Al-Bukhaiti, M.A.; Mohamad, A.A.K.; Emara, K.M.; Ahmed, S.M. Effect of slurry concentration on erosion wear behavior of AISI 5117 steel and high-chromium white cast iron. *Ind. Lubr. Tribol.* **2018**, *70*, 628–638. [CrossRef]
148. Gelfi, M.; Pola, A.; Girelli, L.; Zacco, A.; Masotti, M.; La Vecchia, G.M. Effect of heat treatment on microstructure and erosion resistance of white cast irons for slurry pumping applications. *Wear* **2019**, *428*, 438–448. [CrossRef]
149. Walker, C.I.; Goulas, A. Performance characteristics of centrifugal pumps when handling non-Newtonian homogeneous slurries. *Proc. Inst. Mech. Eng. Part A Power Process Eng.* **1984**, *198*, 41–49. [CrossRef]
150. Walker, C.I.; Robbie, P. Comparison of some laboratory wear tests and field wear in slurry pumps. *Wear* **2013**, *302*, 1026–1034. [CrossRef]
151. Xie, Y.; Jiang, J.J.; Tufa, K.Y.; Yick, S. Wear resistance of materials used for slurry transport. *Wear* **2015**, *332*, 1104–1110. [CrossRef]
152. Jones, M.; Llewellyn, R.J. Erosion–corrosion assessment of materials for use in the resources industry. *Wear* **2009**, *267*, 2003–2009. [CrossRef]
153. Pitt, C.H.; Chang, Y.M. Jet slurry corrosive wear of high-chromium cast iron and high-carbon steel grinding ball alloys. *Corrosion* **1986**, *42*, 312–317. [CrossRef]
154. Correa, R.; Bedolla-Jacuinde, A.; Zuno-Silva, J.; Cardoso, E.; Mejía, I. Effect of boron on the sliding wear of directionally solidified high-chromium white irons. *Wear* **2009**, *267*, 495–504. [CrossRef]
155. Gundlach, R.B.; Parks, J.L. Influence of abrasive hardness on the wear resistance of high chromium irons. *Wear* **1978**, *46*, 97–108. [CrossRef]
156. Penagos, J.J.; Ono, F.; Albertin, E.; Sinatora, A. Structure refinement effect on two and three-body abrasion resistance of high chromium cast irons. *Wear* **2015**, *340*, 19–24. [CrossRef]
157. Deshpande, R.J.; Natarajan, K.A. Studies on grinding media wear and its effect on flotation of ferrugenous phosphate ore. *Miner. Eng.* **1999**, *12*, 1119–1125. [CrossRef]
158. Chen, G.L.; Tao, D.; Parekh, B.K. A laboratory study of high chromium alloy wear in phosphate grinding mill. *Int. J. Miner. Process.* **2006**, *80*, 35–42. [CrossRef]
159. Ribeiro, L.; Barbosa, A.; Viana, F.; Baptista, A.M.; Dias, C.; Ribeiro, C.A. Abrasion wear behaviour of alloyed and chilled cast irons. *Wear* **2011**, *270*, 535–540. [CrossRef]
160. Rajagopal, V.; Iwasaki, I. Corrosion properties of cast iron ball materials in wet grinding. *Corrosion* **1992**, *48*, 124–131. [CrossRef]
161. Stachowiak, G.B.; Stachowiak, G.W.; Celliers, O. Ball-cratering abrasion tests of high-Cr white cast irons. *Tribol. Int.* **2005**, *38*, 1076–1087. [CrossRef]
162. Anijdan, S.H.M.; Bahrami, A.; Varahram, N.; Davami, P. Effects of tungsten on erosion–corrosion behavior of high chromium white cast iron. *Mater. Sci. Eng. A* **2007**, *454*, 623–628. [CrossRef]
163. Albright, D.L.; Dunn, D.J. Wear behavior of iron and steel castings for the mining industry. *JOM* **1983**, *35*, 23–29. [CrossRef]
164. Chenje, T.W.; Simbi, D.J.; Navara, E. Wear performance and cost effectiveness—-a criterion for the selection of grinding media for wet milling in mineral processing operations. *Miner. Eng.* **2003**, *16*, 1387–1390. [CrossRef]
165. Gundewar, C.S.; Natarajan, K.A.; Nayak, U.B.; Satyanarayana, K. Studies on ball wear in the grinding of Kudremukh hematite-magnetite ore. *Miner. Eng.* **1990**, *3*, 207–220. [CrossRef]

Disclaimer/Publisher's Note: The statements, opinions and data contained in all publications are solely those of the individual author(s) and contributor(s) and not of MDPI and/or the editor(s). MDPI and/or the editor(s) disclaim responsibility for any injury to people or property resulting from any ideas, methods, instructions or products referred to in the content.